Numerical Simulation of Microfiltration of Oil-in-Water Emulsions

By:
Tohid Darvishzadeh

Advisor:
Dr. Nikolai Priezjev

Department of Mechanical Engineering
Michigan State University

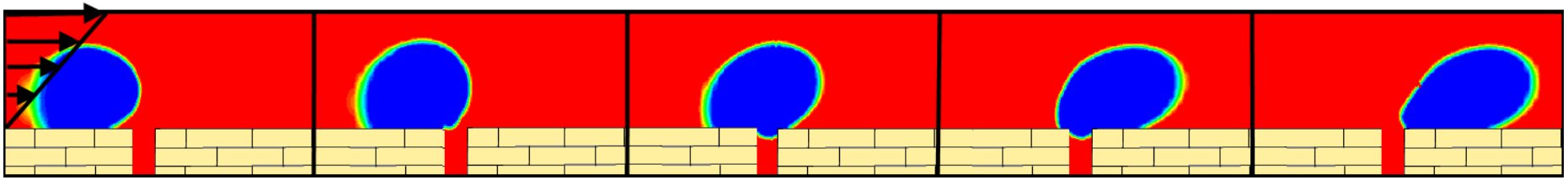

•**T. Darvishzadeh, V.V. Tarabara, N.V. Priezjev, *Journal of Membrane Science*, 447, 442-451 (2013).**
•**T. Darvishzadeh, N.V. Priezjev, *Journal of Membrane Science*, 423-424, 468-476 (2012).**
•**T. Darvishzadeh, B. Bhattarai, N.V. Priezjev, *Journal of Membrane Science*, 563, 610 (2018).**

MICHIGAN STATE UNIVERSITY

Outline

- Introduction
- Results
  - Part 1:
    - Oil film entry into pores of arbitrary shape (effect of transmembrane pressure).
    - Oil drop entry dynamics into circular pores under shear flow (effect of shear rate and transmembrane pressure).
  - Part 2:
    - Effect of confinement on drop dynamics.
    - Effect of viscosity ratio on drop dynamics.
    - Effect of surface tension coefficient on drop dynamics.
    - Effect of contact angle on drop dynamics.
    - Effect of drop size on drop dynamics.
- Conclusions
- Proposed future work

Microfluidics: Characteristics and Applications

Fluid flow at micron-scales.

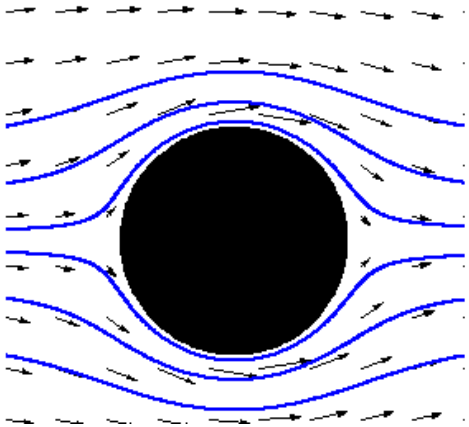

❖Laminar flow (small Re)

❖High surface to volume ratio.

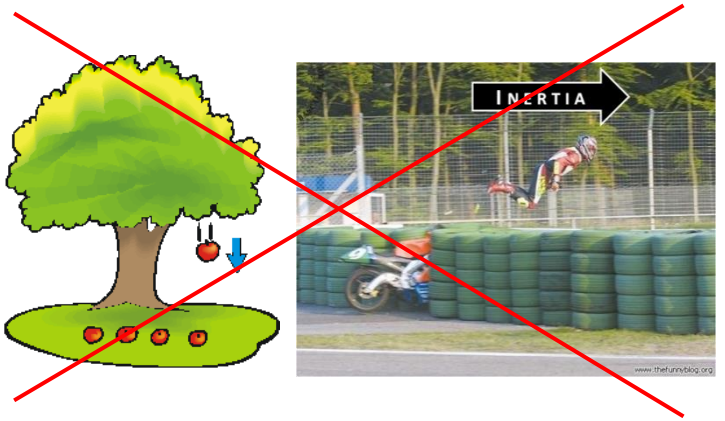

❖Negligible gravity and inertia.

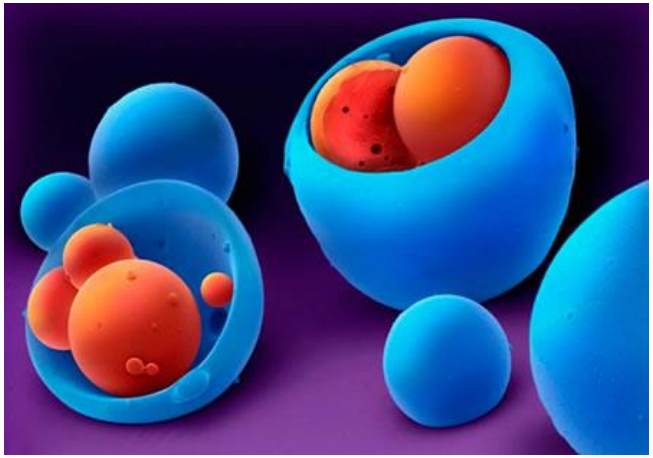

❖Encapsulation of molecules, bio-reagents, and cells for delivery or reaction.

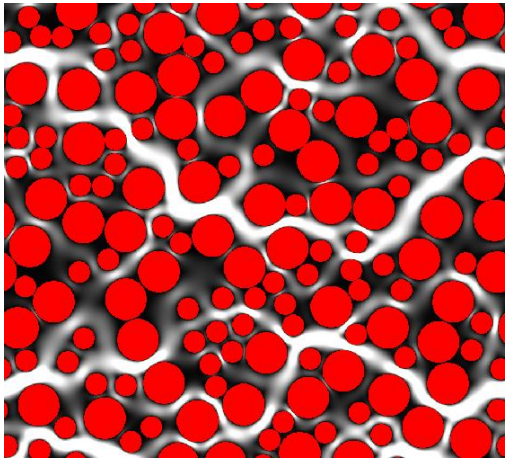

❖Flow through porous media (e.g. oil extraction)

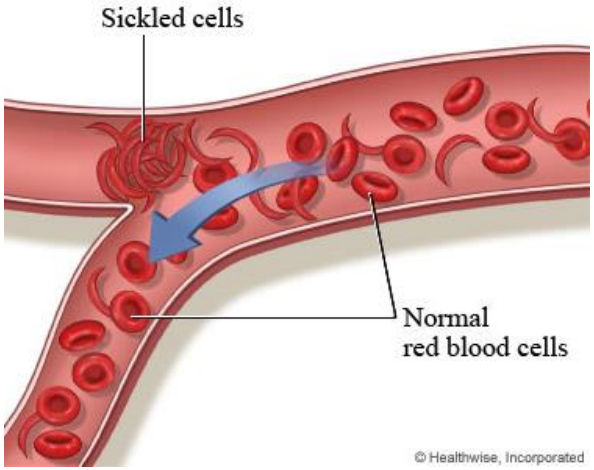

❖Biological flows (e.g. flow inside blood vessels)

Emulsions: Properties and Applictions

Mixture of two immiscible fluids

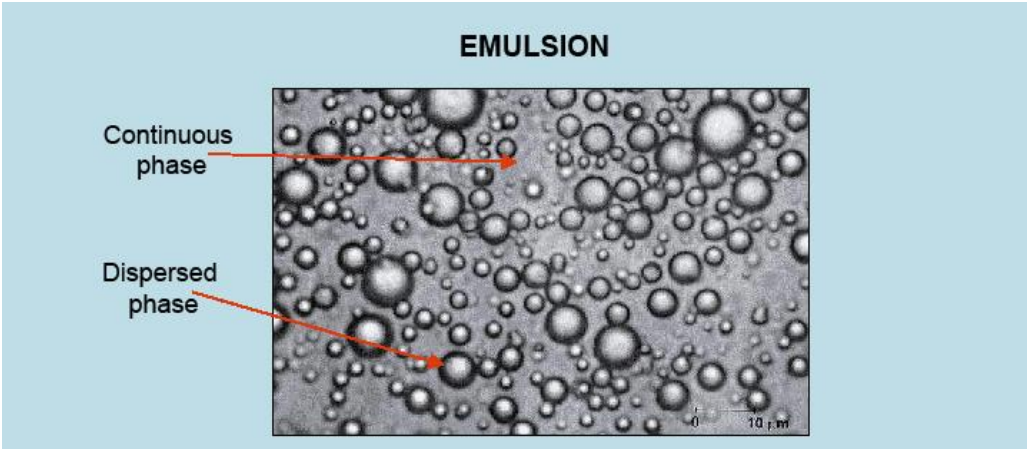

❖Dispersed droplets in continuous phase.

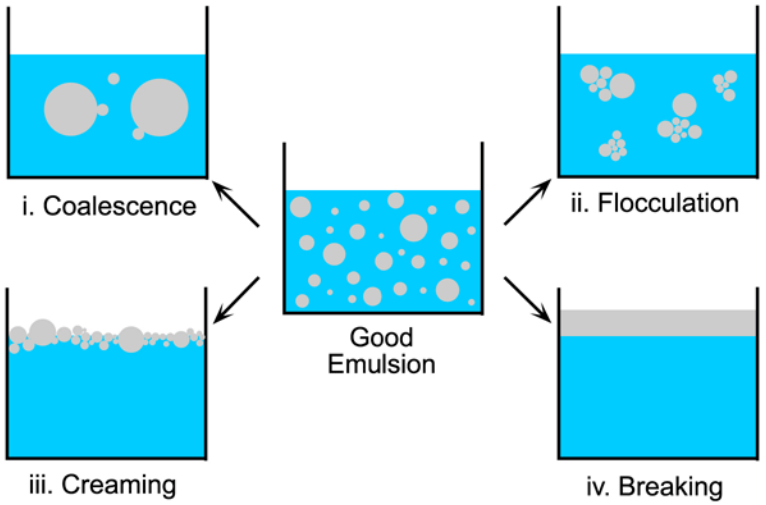

❖Various forms of Immiscible fluids

❖Beneficial emulsion production: food (left) & oil transportation (right).

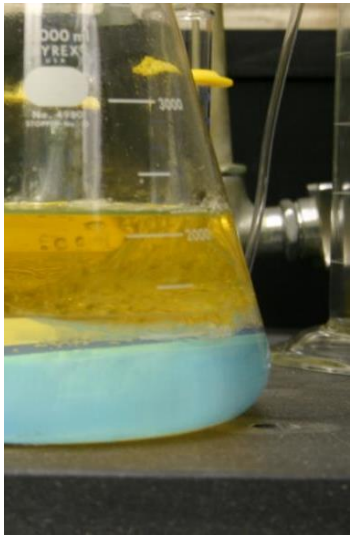

❖Unfavorable emulsion production: industrial wastewater (left) & biodiesel washing (right).

Emulsions: Production and Separation

❑Mixture of two-immiscible fluid

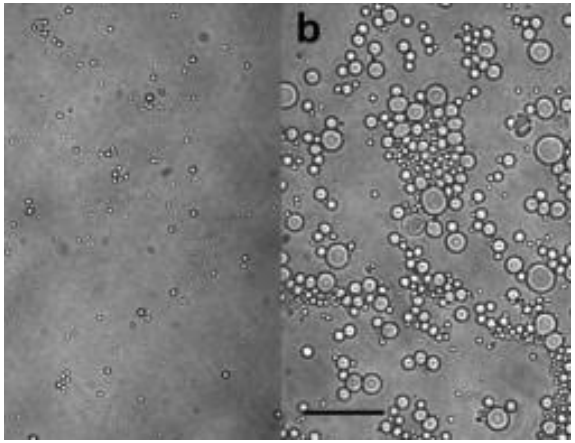

❖Ultrasound emulsification

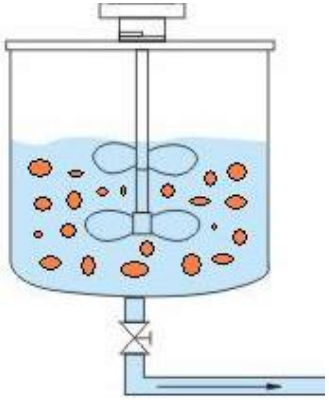

❖Mechanical agitation

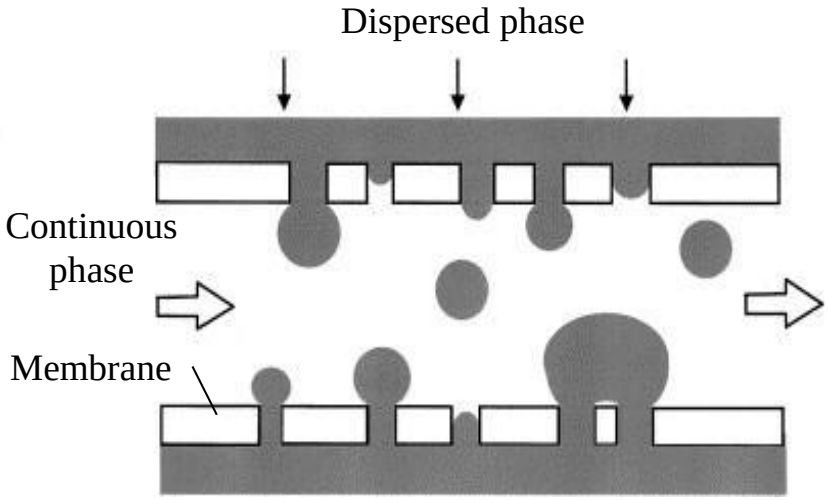

❖Membrane emulsification

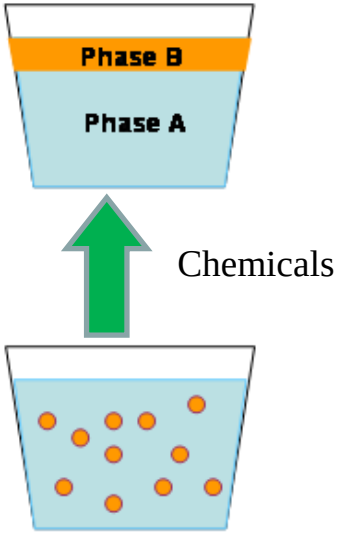

❖Chemical Demulsification

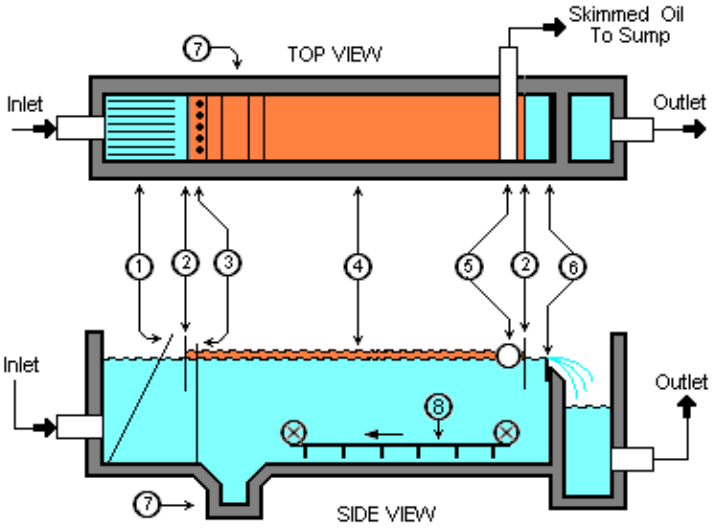

❖Gravity separator

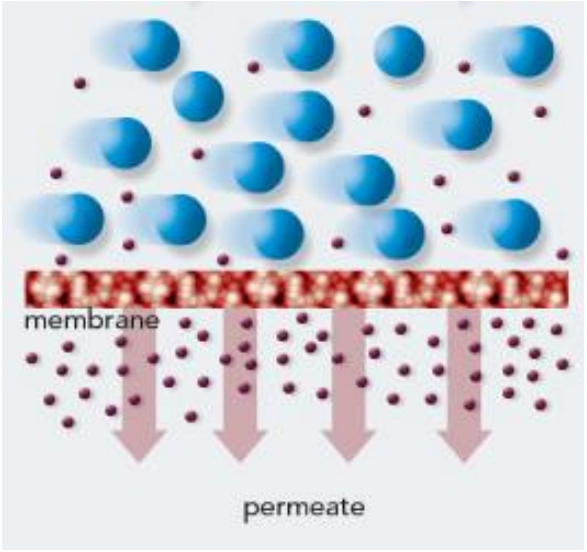

❖Membrane microfiltration

Microfiltration of oil: Motivations and Methods

❖Oil spill in the Gulf of Mexico.

❖Industrial wastewater in Thailand.

❖Cutting fluids for machining.

Oil-Water Separation Methods

Centrifuge separation

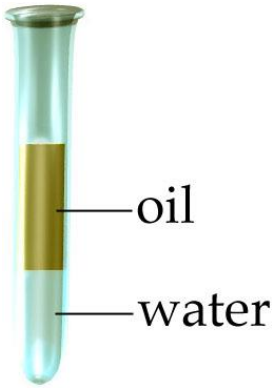

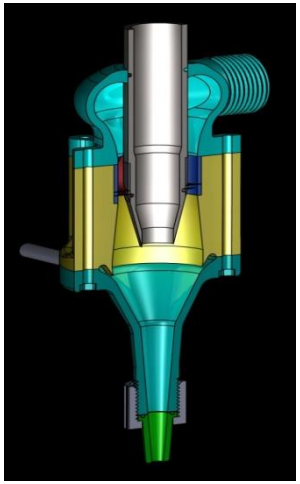

Hydrocyclone

Membrane filtration

Dead-End

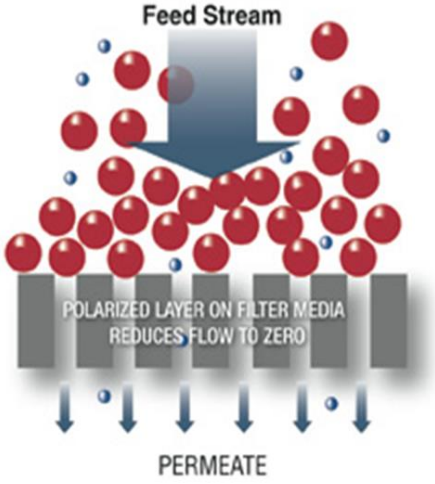

Crossflow

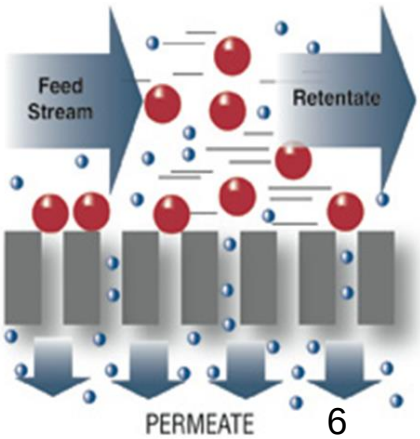

Membrane Fouling, Permeate Flux, and Pore Shape

❖ Optimum design: high water flux and high oil **rejection**.

❖ Major issue: **Fouling** reduces **Water flux** in time.

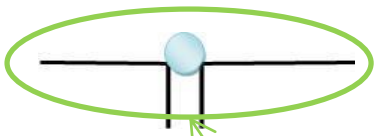

Complete Blocking: *happens at the initial stages of filtration. A droplet blocks the pore completely*

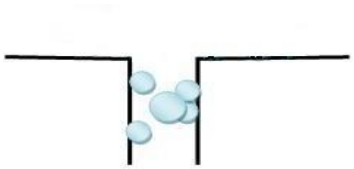

Standard blocking: *deposition of drops inside the pore.*

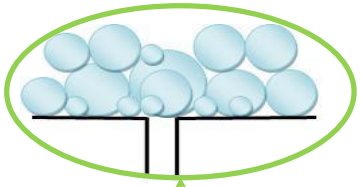

Cake Formation: *happens at the final stages of filtration. A layer of drops forms on the surface.*

Circular Pores

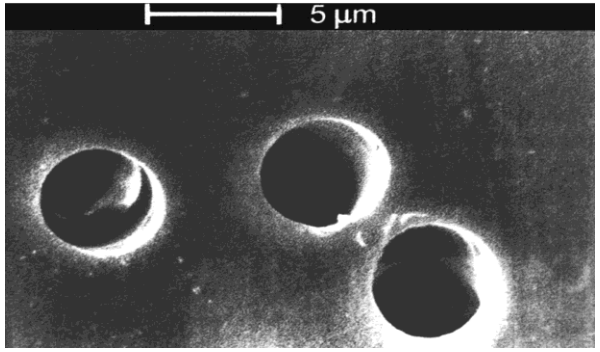

Slotted Pores

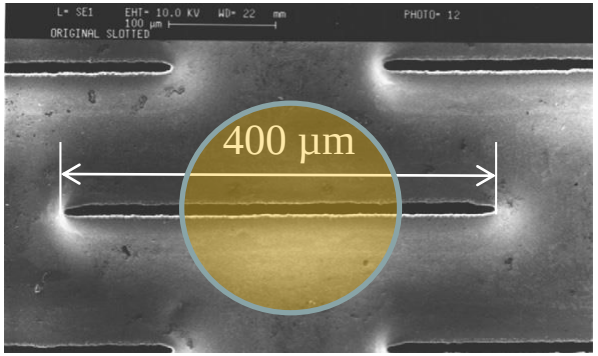

Flux decline in crossflow microfiltration.

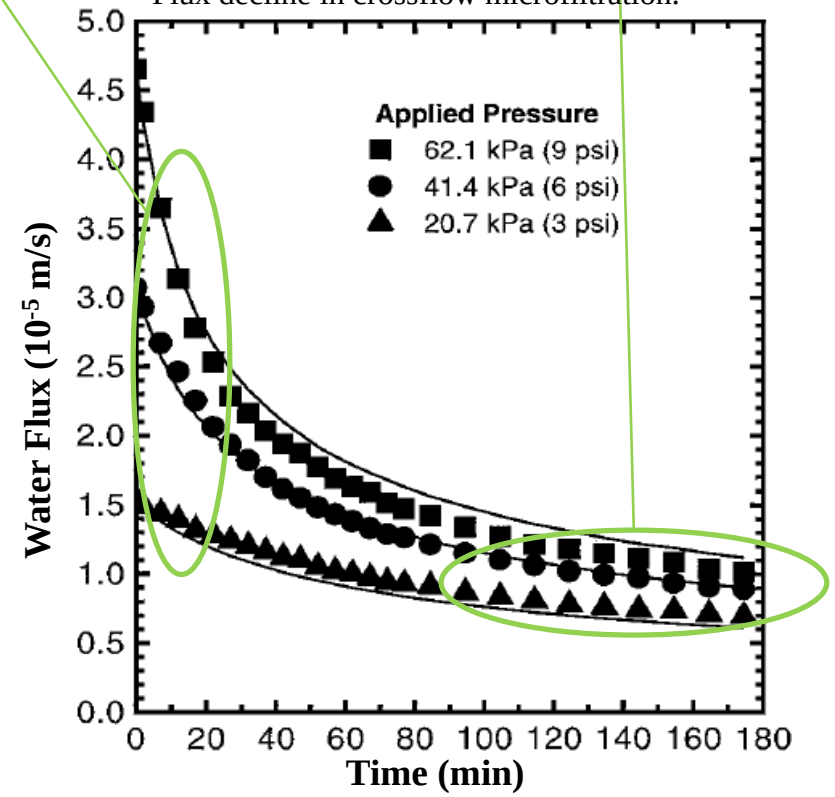

❖Slotted pores: **higher flux rates** than circular pores due to **lower fouling rate**.

Critical Pressure of Permeation

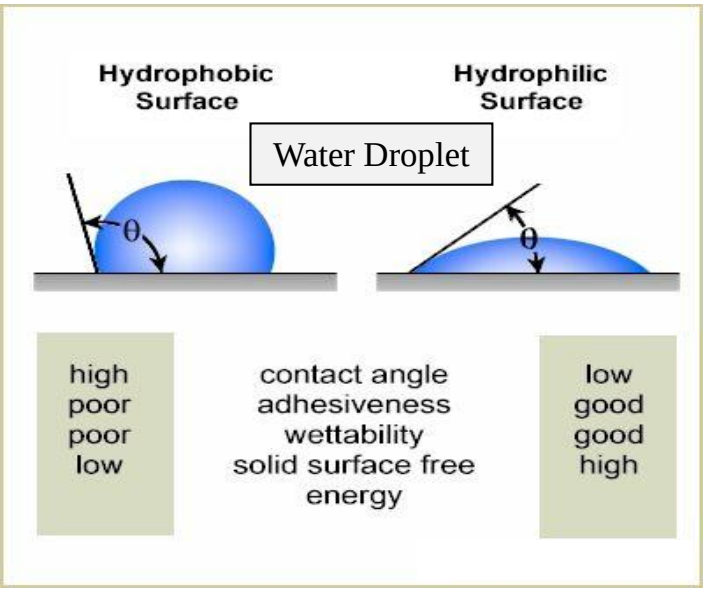

Young-Laplace Equation: pressure drop across an interface:

$$\Delta P = \sigma \cos\theta \left(\frac{1}{R_x} + \frac{1}{R_y} \right)$$

For a spherical interface:

$$\Delta P = 2\sigma \cos\theta \left(\frac{1}{R_d} \right)$$

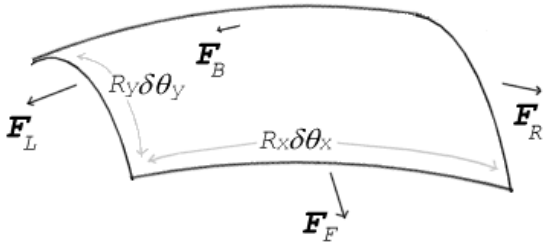

Critical Pressure of Permeation: Pressure required to permeate the dispersed fluid.

$R_{pore} \uparrow \Rightarrow P_{crit} \downarrow$

$R_{drop} \uparrow \Rightarrow P_{crit} \uparrow$

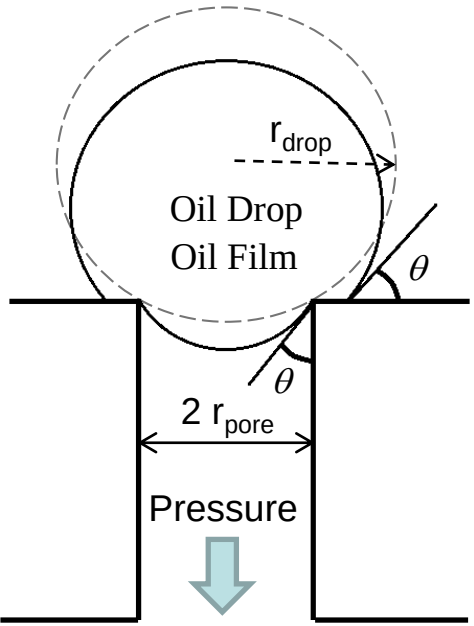

Critical pressure for a droplet deposited on a circular pore:

$$P_{crit} = 2\sigma \frac{\cos(\theta)}{r_{pore}} \times \left[1 - \left\{ \frac{2 + 3\cos\theta - \cos^3\theta}{4\left(\frac{r_{drop}}{r_{pore}}\right)^3 \cos^3\theta - (2 - 3\sin\theta + \sin^3\theta)} \right\}^{1/3} \right]$$

F.F. Nazzal and M.R. Wiesner, Water Environ. Res. (1996).

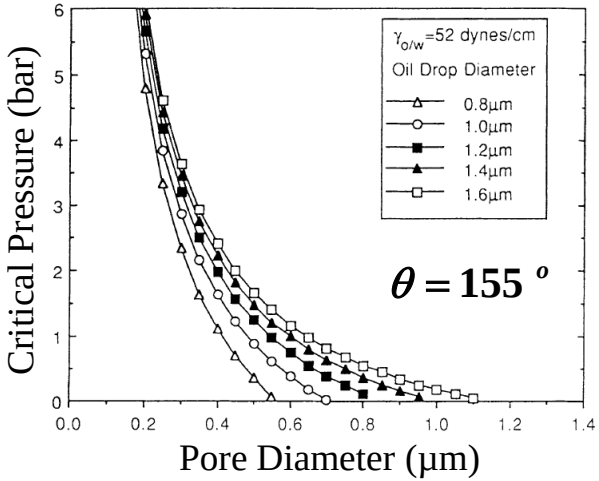

❖Critical pressure as a function of drop size and pore size.

Crossflowing Systems: Confined vs. Unconfined

Confined (T-junction)

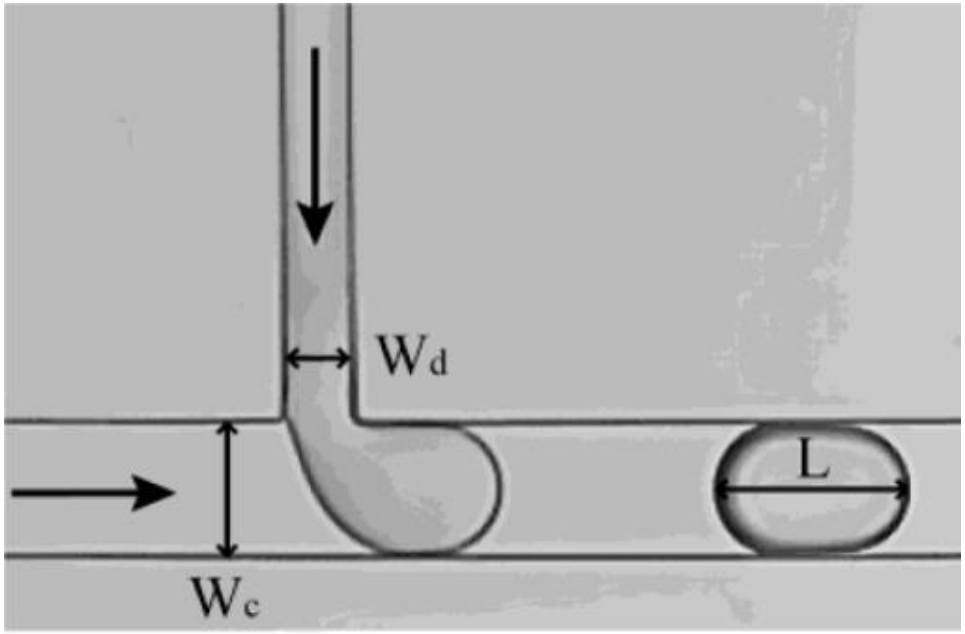

Unconfined

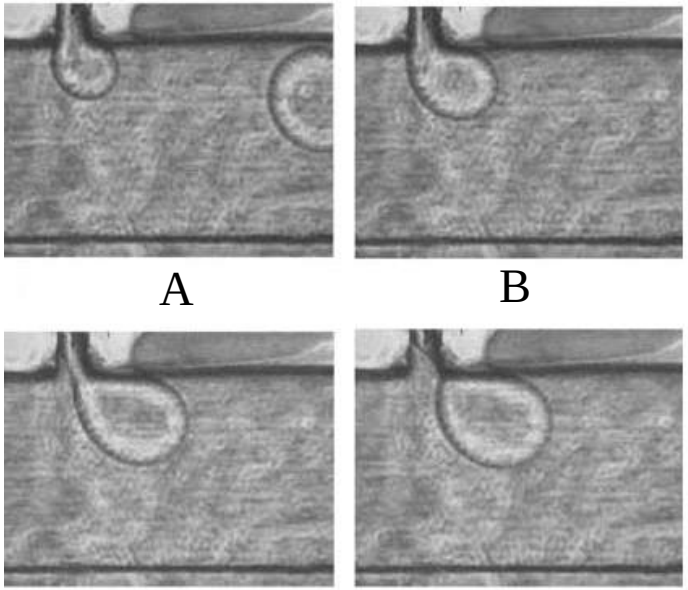

	Confined	Unconfined
Channel driving force	Pressure	Shear stress
Deformation and breakup	Due to pressure gradient	Due to shear stress and pressure.
Dispersion	Plugs	Droplets
Continuous phase flow rate	Very Low	high
Geometry	Strongly dependent on channel size	Roughly independent of channel size.
Droplets size	Easily controllable (mono-disperse)	Hardly controllable (poly-disperse)

Numerical Method and Important Parameters

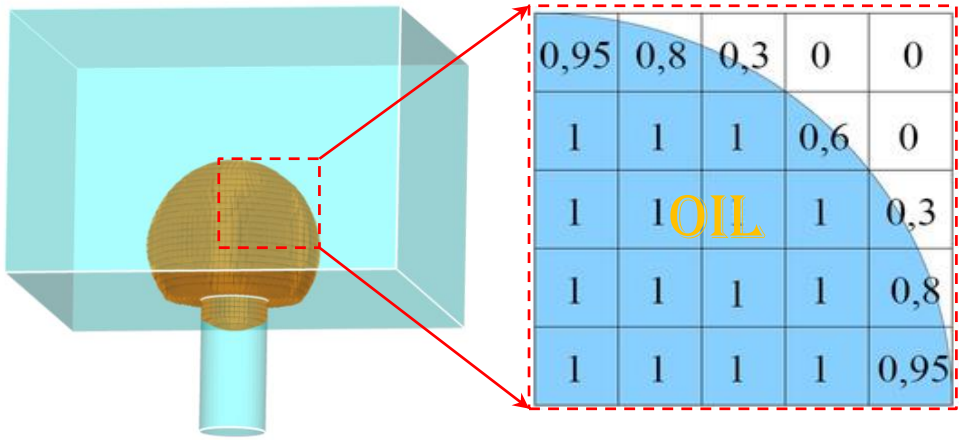

- ❖CFD: Inexpensive, repeatable, instructive.
- ❖Flow solver: **FLUENT**
- ❖3D interface tracking: **Volume of Fluid**
- ❖Interface: outlined by cells containing both phases.
- ❖ Surface Tension: "Continuum Surface Force"

Governing Equations

Continuity

$$\frac{1}{\rho_q}\left[\frac{\partial}{\partial t}\left(\alpha_q\rho_q\right)+\nabla\cdot\left(\alpha_q\rho_q\vec{v}_q\right)=S_{\alpha_q}+\sum_{p=1}^{n}\left(\dot{m}_{pq}-\dot{m}_{qp}\right)\right]$$

Compatibility

$$\rho=\alpha_2\rho_2+(1-\alpha_2)\rho_1$$

Momentum

$$\frac{\partial}{\partial t}\left(\rho\vec{v}\right)+\nabla\cdot\left(\rho\vec{v}\vec{v}\right)=-\nabla p+\nabla\cdot\left[\mu\left(\nabla\vec{v}+\nabla\vec{v}^{T}\right)\right]+\rho\vec{g}+\vec{F}$$

Important Parameters	
Viscosity Ratio (oil to water)	λ
Surface Tension Coefficient	σ
Contact angle (measured in oil)	θ
Shear Rate	$\dot{\gamma}$
Drop to pore size ratio	r_d / r_p

Validation of the Numerical Simulation

$\rho_1 = \rho_2 = 1$, $\mu_1 = \mu_2 = 1$, $r_d = 0.25$, Shear = 1, Re = 0.0625

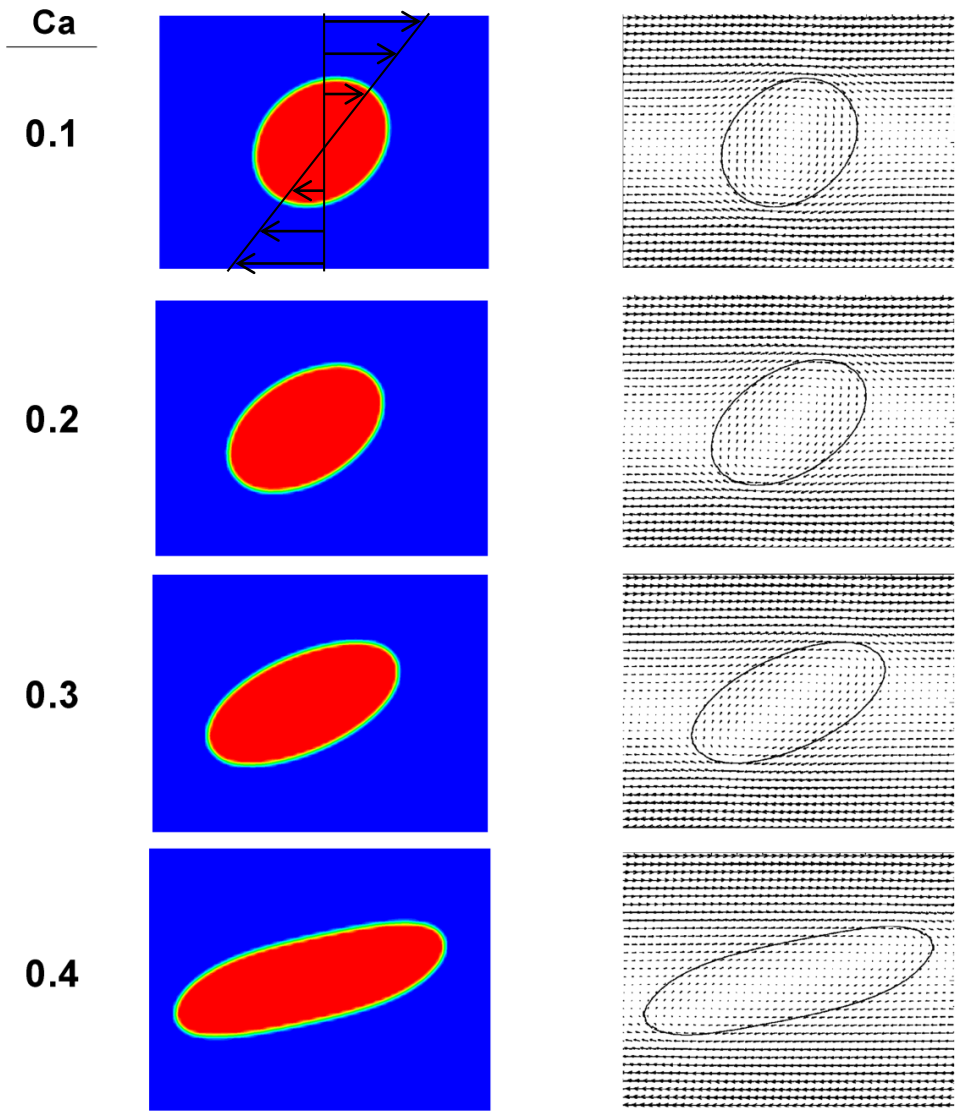

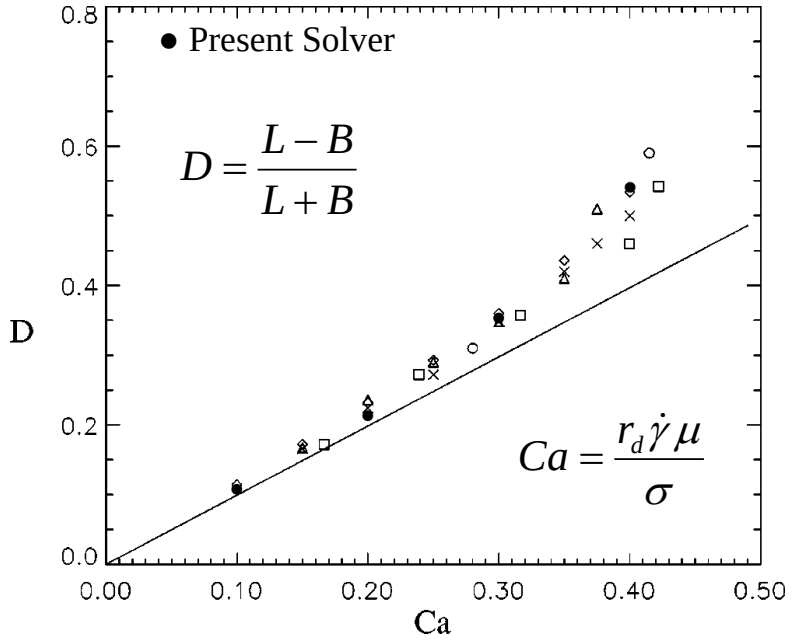

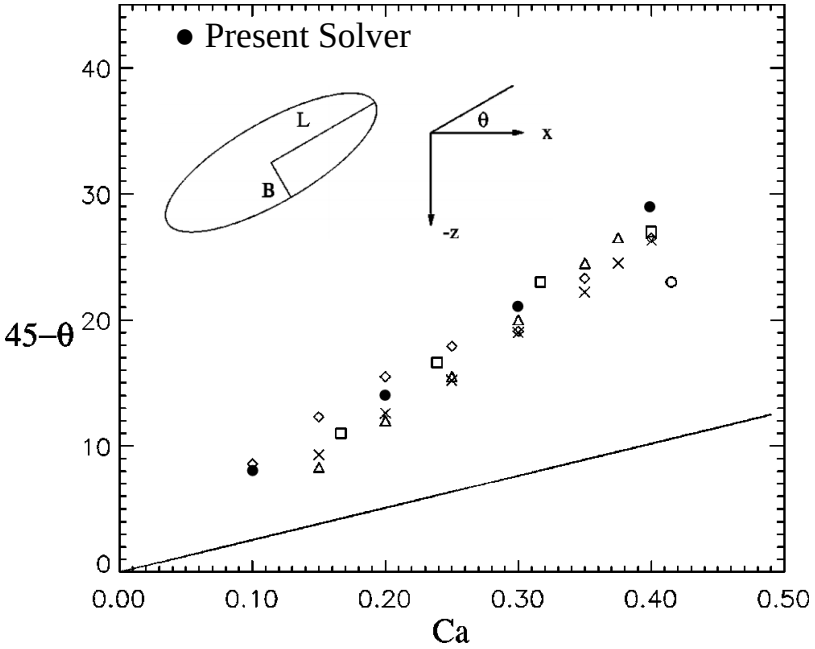

† J. Li, Y.Y. Renardy, M. Renardy, Phys. Fluids **12** (2000) 269

Results

- **Part 1:**

1. **Oil film permeation into pores of arbitrary cross-section (effect of transmembrane pressure).**
2. Oil drop entry dynamics into circular pores under shear flow.

Critial Pressure of Permeation of Liquid Films inside Pores of Arbitrary Cross-Section

❖Young-Laplace (pressure vs surface tension):

$$\Delta P = 2\sigma\kappa$$

❖Mean curvature (no gravity) for arbitrary surface *z:*

$$2\kappa = \nabla \cdot \left(\frac{\nabla z}{\sqrt{1+|\nabla z|^2}} \right)$$

❖Boundary condition (imposed contact angle):

$$\cos\theta = \vec{n} \cdot \left(\frac{\nabla z}{\sqrt{1+|\nabla z|^2}} \right)$$

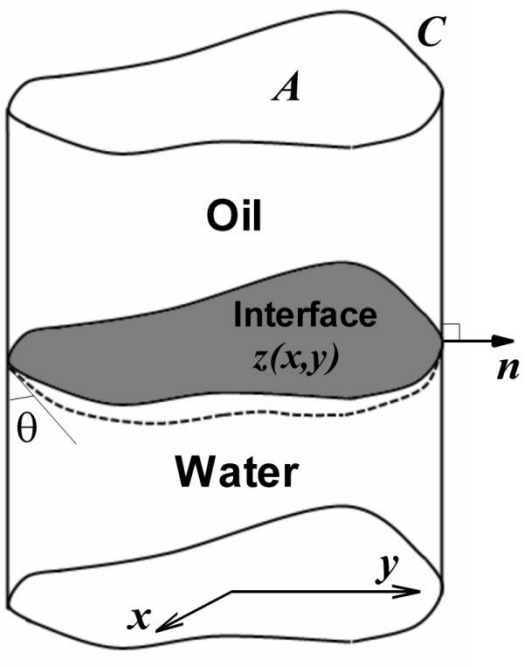

C_p : pore circumference

A_p : pore CS area

Integrating over cross-section

$$2\kappa = \frac{C_p \cos\theta}{A_p}$$

Young-Laplace

$$P_{crit} = \frac{\sigma C_p \cos\theta}{A_p}$$

Numerical Simulation of Thin Oil Film on a Rectangular Pore

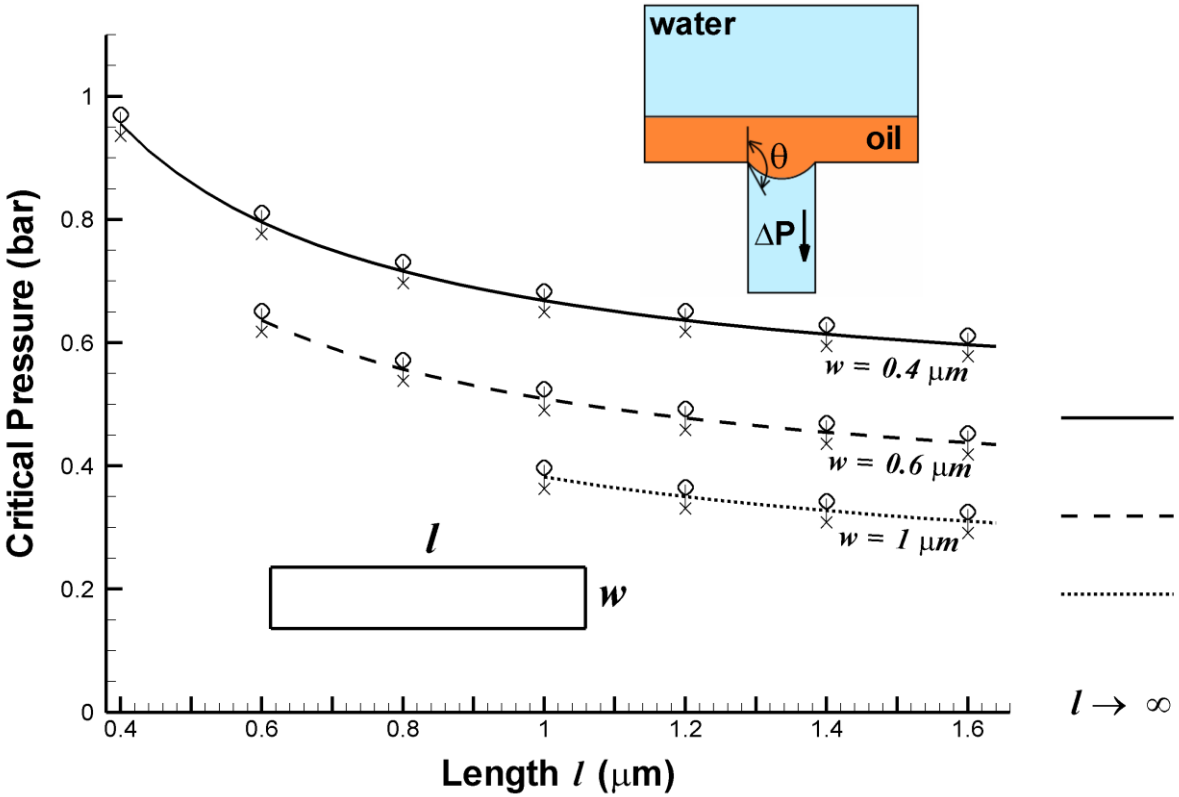

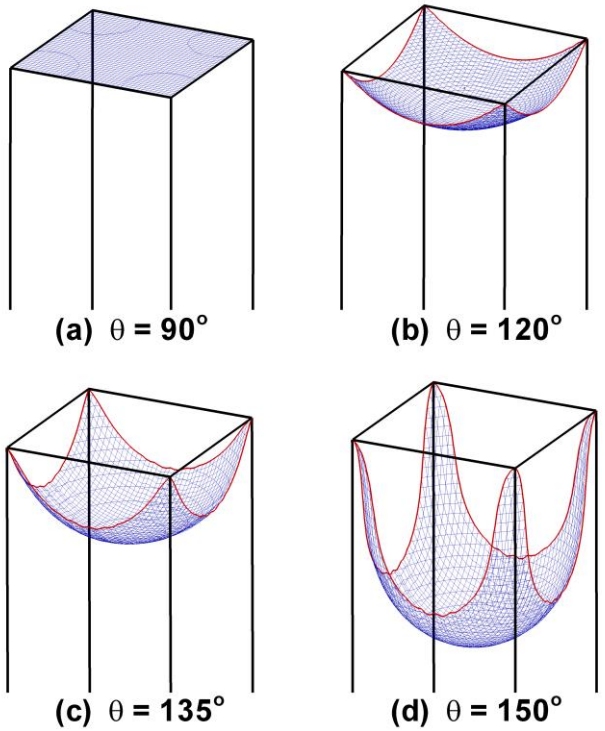

λ = 2.45, σ = 19.1 mN/m, θ = 120°

$$2\kappa = \nabla \cdot \left(\frac{\nabla z}{\sqrt{1 + |\nabla z|^2}} \right)$$

- Lower aspect ratio: higher critical pressure.
- Excellent agreement with critical pressure formula.
- For square cross-section interface is spherical.
- For 90 degrees: zero curvature + zero pressure gradient.
- For 150 degrees no steady shape. Corners pinned.

$$P_{crit} = 2\sigma \cos\theta \left(\frac{1}{w} + \frac{1}{l} \right)$$

Numerical Simulation of Thin Oil Film on an Elliptical Pore

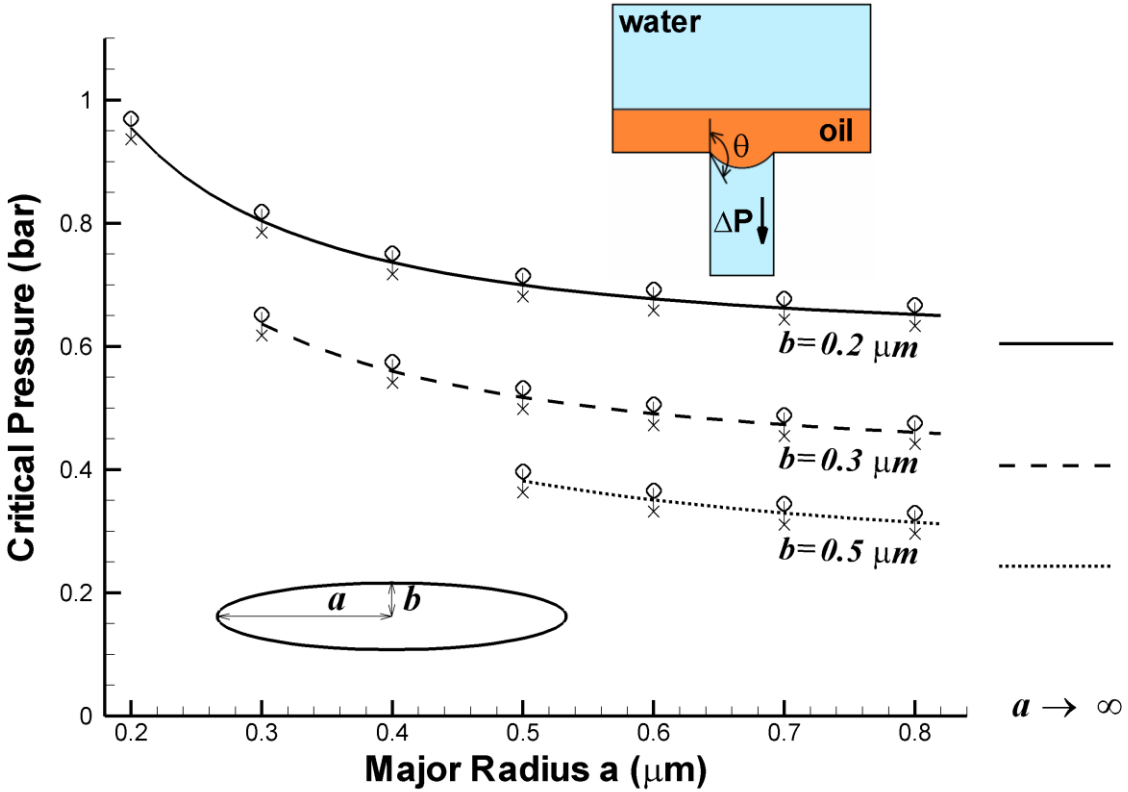

λ = 2.45, σ = 19.1 mN/m, θ = 120°

❖Excellent agreement with critical pressure formula.

❖Infinitely long ellipse: higher critical pressure than infinitely long rectangle.

❖If aspect ratio > *1.635* there is a critical contact angle above which the interface cannot remain attached.

❖Interface inside an elliptical pore is not spherical.

Using Ramanujan's formula for ellipse perimeter (0.04% error):

$$h = \frac{(a-b)^2}{(a+b)^2}$$

$$P_{crit} \approx \frac{(a+b)}{ab}\left[1 + \frac{3h}{10+\sqrt{4-3h}}\right]\sigma\cos\theta$$

Results

- **Part 1:**

1. Oil film permeation into pores of arbitrary cross-section.
2. **Oil drop entry dynamics into circular pores under shear flow (effect of shear rate and transmembrane pressure).**

Numerical Simulation of Oil Droplet on a Circular Pore with No Crossflow

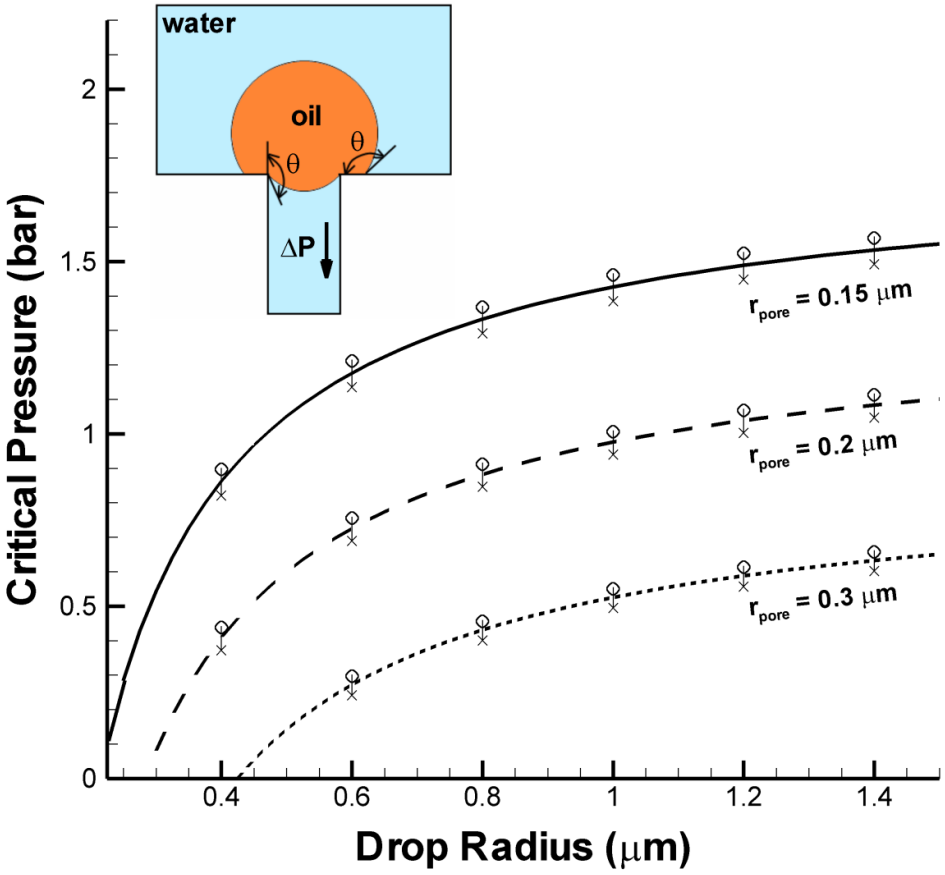

λ = 2.45, σ = 19.1 mN/m, θ = 135°

Note: If contact angle is 90 degrees, the predicted critical pressure is negative, meaning that the drop will penetrate the pore in the absence of transmembrane pressure.

- Excellent agreement with critical pressure formula.
- Critical pressure increases with drop size and decreases with pore size.
- Drop entry dynamics inside pore slows down significantly when approaching critical pressure.
- Critical pressure of an infinitely large drop corresponds to an infinite oil film.

$$P_{crit} = 2\gamma \frac{\cos(\theta)}{r_{pore}} \times \left[1 - \left\{ \frac{2 + 3\cos\theta - \cos^3\theta}{4\left(\frac{r_{drop}}{r_{pore}}\right)^3 \cos^3\theta - (2 - 3\sin\theta + \sin^3\theta)} \right\}^{1/3} \right]$$

F.F. Nazzal and M.R. Wiesner, Water Environ. Res. (1996).

Computational setup for sheared droplet on membrane surface with a circular pore

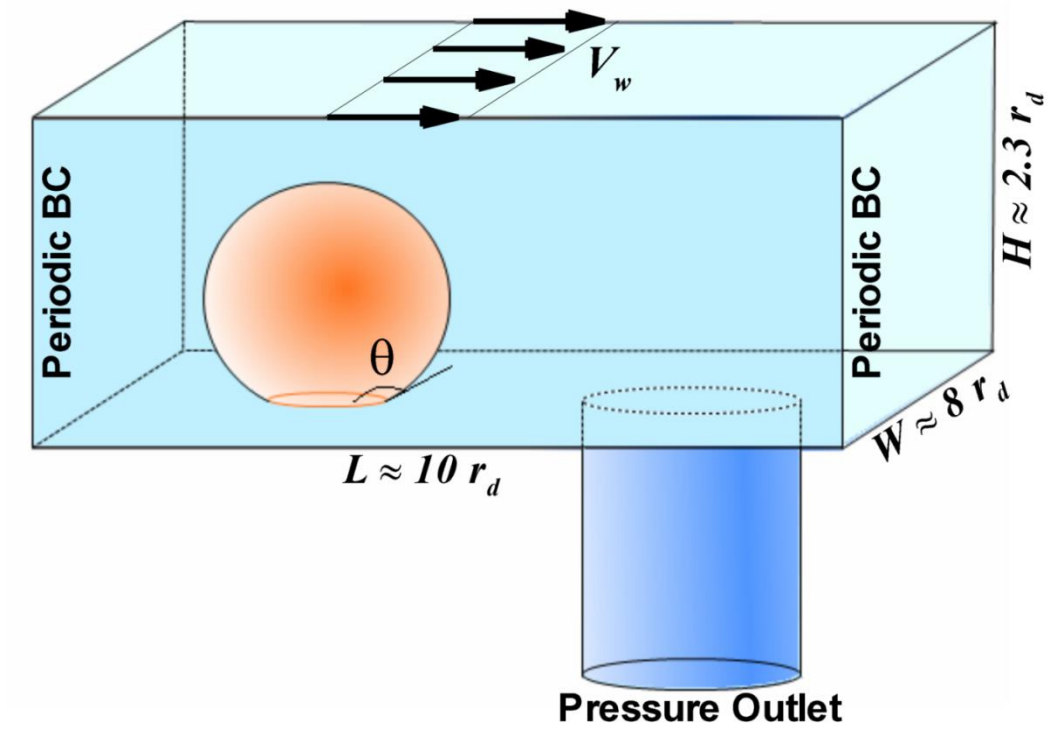

❖Channel dimensions chosen to minimize finite size effects.

❖Moving top wall induces linear shear flow.

❖Pressure outlet at the bottom of pore controls transmembrane pressure.

❖Periodic boundary condition to ensure accurate shear flow.

$$Ca = \frac{\mu \dot{\gamma} r_d}{\sigma} \leq 0.03 \qquad \mathrm{Re} = \frac{\rho_w \dot{\gamma} r_d^{\,2}}{\mu_w} \leq 0.5$$

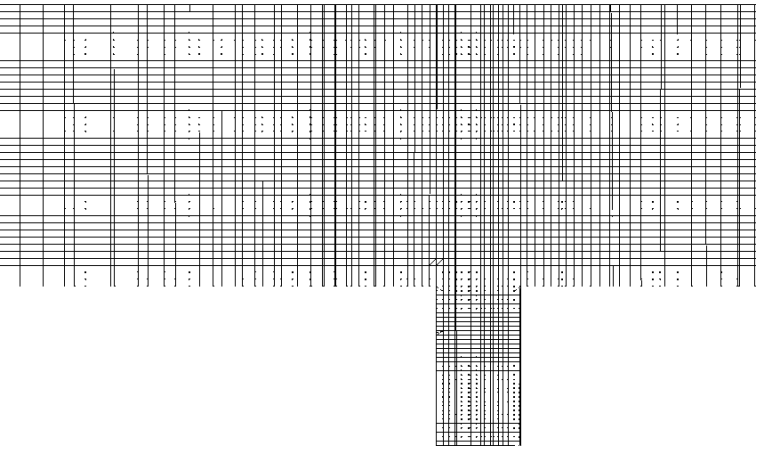

The mesh consists of hexagonal grids and contains 30 cells along pore diameter.

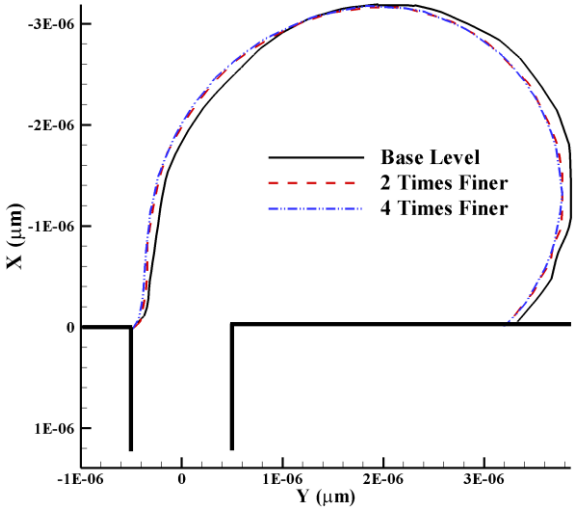

Effect of Transmembrane Pressure and Shear Rate

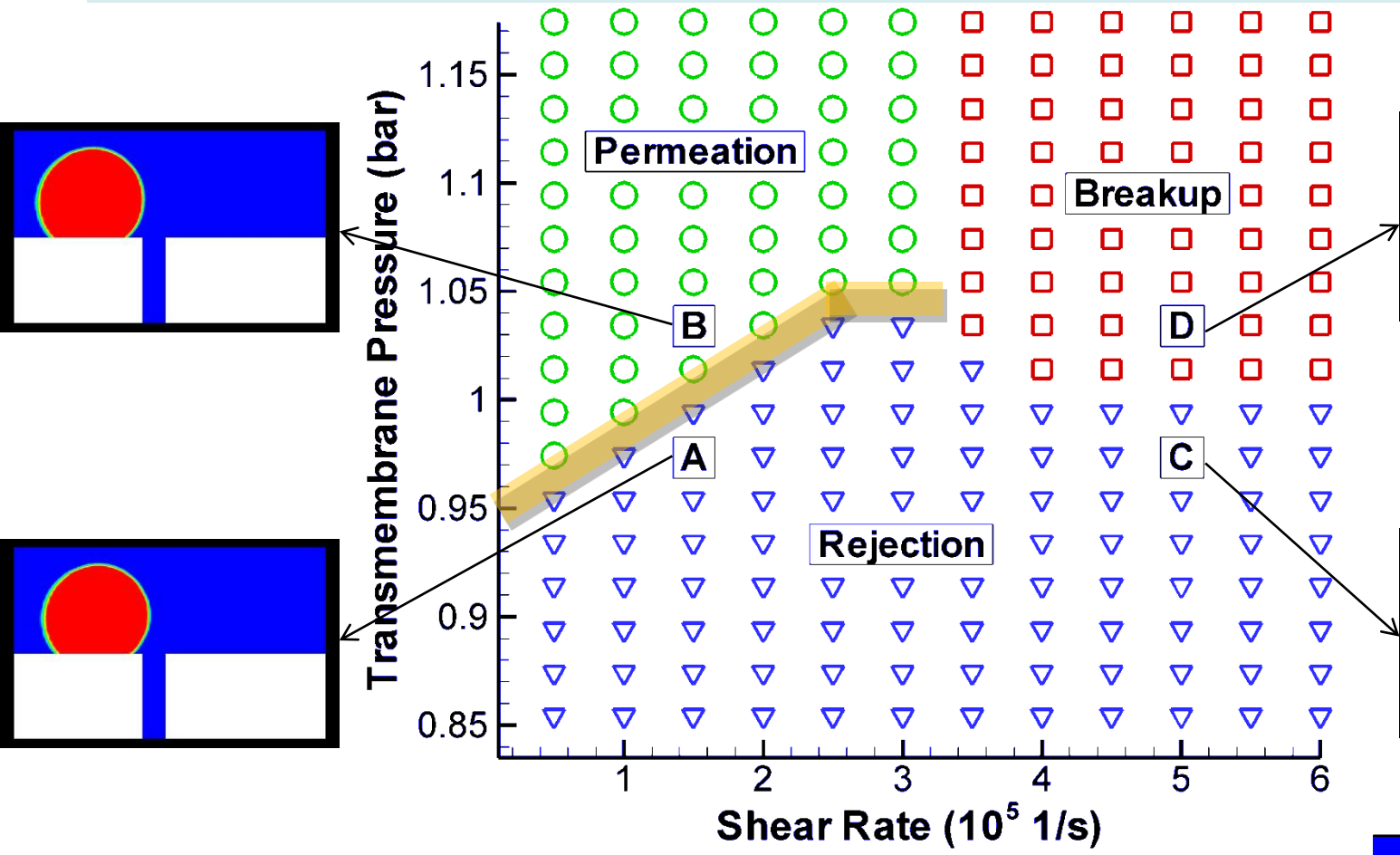

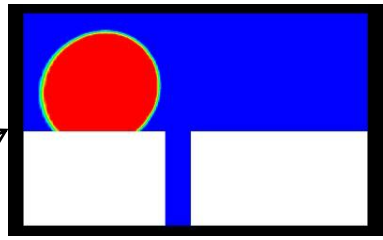

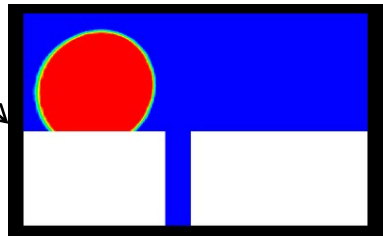

r_{pore} = 0.2 μm, r_{drop} = 0.9 μm, λ = 2.45, σ = 19.1 mN/m, θ = 135°

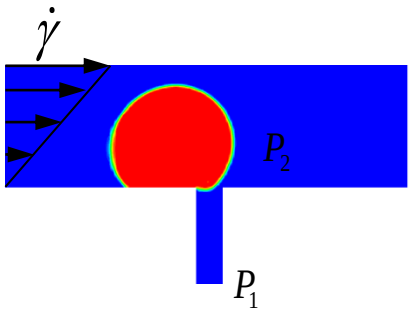

- With increasing shear rate, critical permeation pressure increases.
- Breakup is roughly independent of the transmembrane pressure.
- The yellow line denotes the **critical pressure of permeation** (Focus of **Part 2**).

T. Darvishzadeh and N.V. Priezjev, *Journal of Membrane Science*, **423-424**, 468-476 (2012).

Leakage Volume with Respect to Transmembrane Pressure

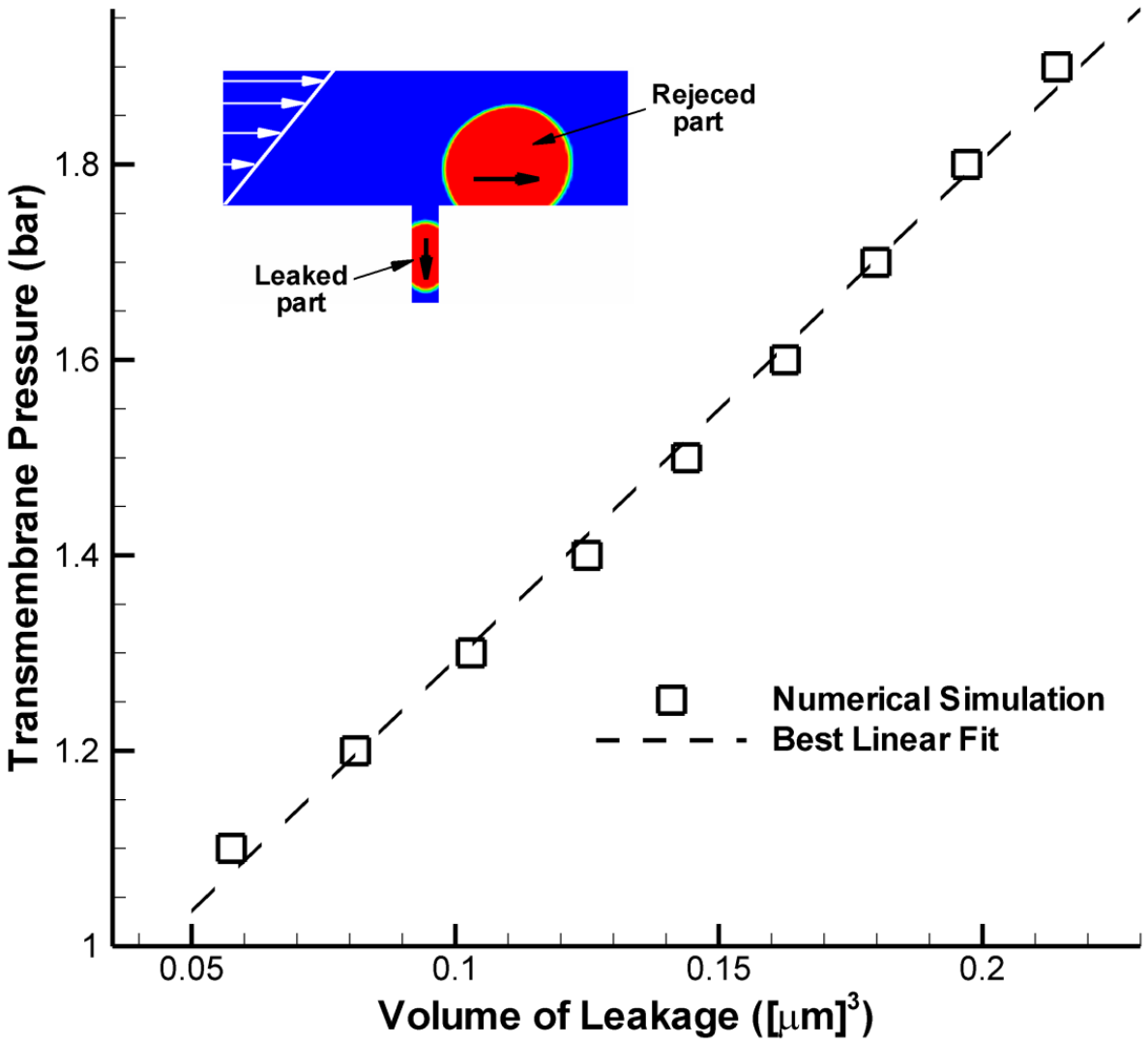

- Volume of leakage: linearly dependent on transmembrane pressure.
- Flow inside pore follows Hagen-Poiseuille.
- For 100% rejection rate breakup should be avoided.

$$\Delta P = \frac{8\mu L Q}{\pi r^4}$$

$$U_{interface} \propto \Delta P$$

r_{pore} = 0.2 μm, r_{drop} = 0.9 μm, λ = 2.45, σ = 19.1 mN/m, θ = 135°, Shear = 5×10^5 s^{-1}

Results

- **Part 2:**

1. **Problem statement.**
2. Effect of confinement on drop dynamics.
3. Effect of viscosity ratio on drop dynamics.
4. Effect of surface tension coefficient on drop dynamics.
5. Effect of contact angle on drop dynamics.
6. Effect of drop size on drop dynamics.

Problem Statement: Interaction of an Oil Droplet with a Membrane Pore

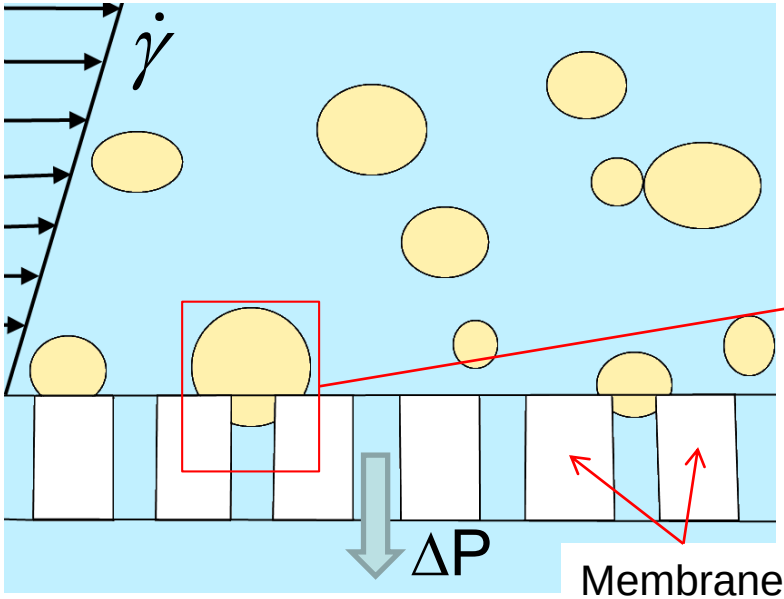

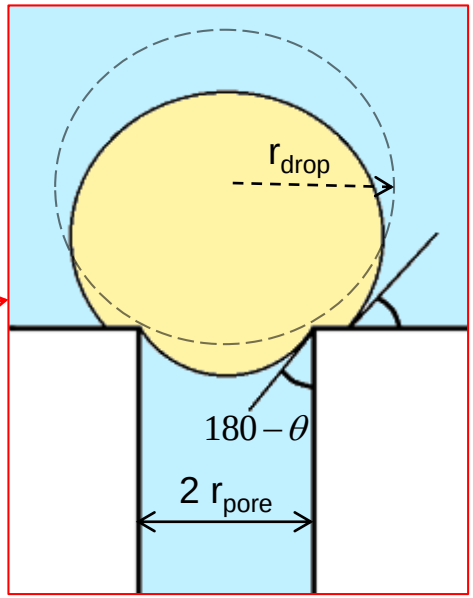

❖Young-Laplace Equation: pressure drop across an interface:

$$\Delta P = 2\kappa\sigma$$

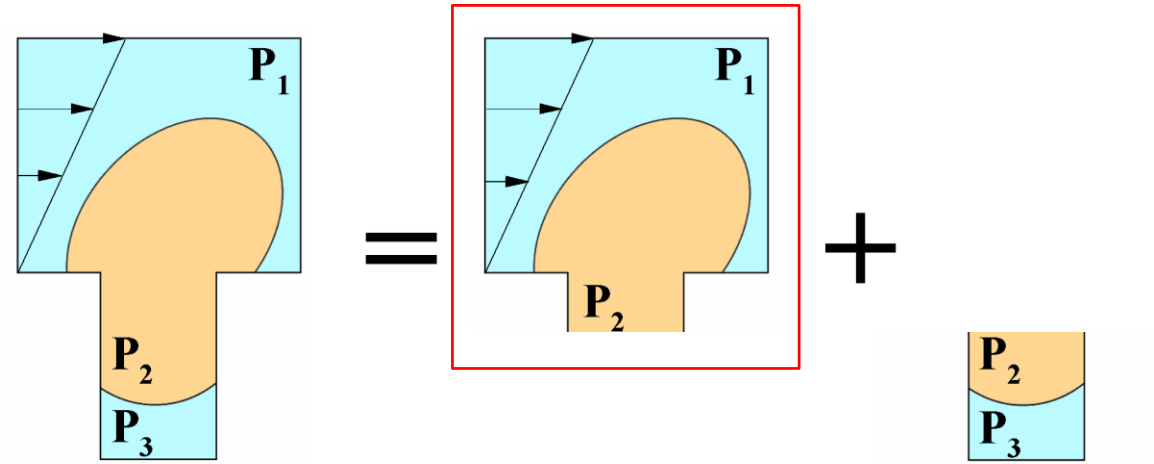

$P_1 - P_3 = P_1 - P_2 + P_2 - P_3$

❖ Motion of interface inside the pore is slow.

❖ The interface inside the channel is highly dynamic.

Analytical formulation: Critical Capillary Number and Critical Pressure

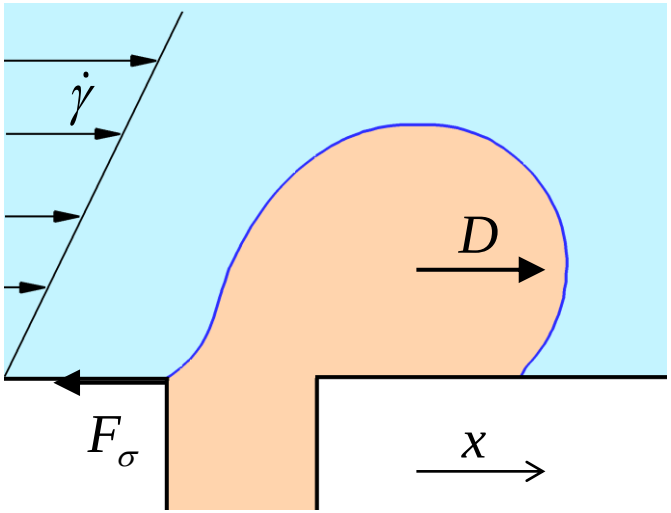

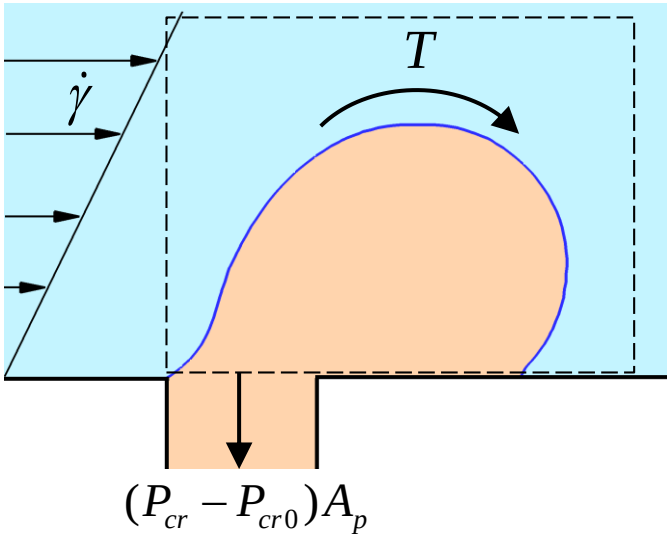

$$D \approx F_\sigma$$

$$T \propto (P_{cr} - P_{cr0}) A_p r_d$$

$$D \propto f_D(\lambda)\mu\dot{\gamma} r_d^{\,2} \qquad F_\sigma \propto \sigma r_p$$

$$T = f_T(\lambda)\pi\mu\dot{\gamma} r_d^{\,3}$$

$$f_D(\lambda) = \frac{2 + 4.51\lambda}{1 + 1.05\lambda}$$

For a hemispherical drop on solid surface†

$$f_T(\lambda) = \frac{2.19\,\lambda}{1 + 0.90\,\lambda}$$

$$Ca_{cr} \propto \frac{1}{f_D(\lambda)\bar{r}}$$

$$\bar{r} = r_d / r_p$$

$$P_{cr} - P_{cr_0} \propto \frac{f_T(\lambda)\sigma\bar{r}Ca}{r_p}$$

† K. Sugiyama, M. Sbragaglia, *J. Eng. Math.* **62,** 35 (2008).

Computational Setup, Boundary Conditions, and Mesh

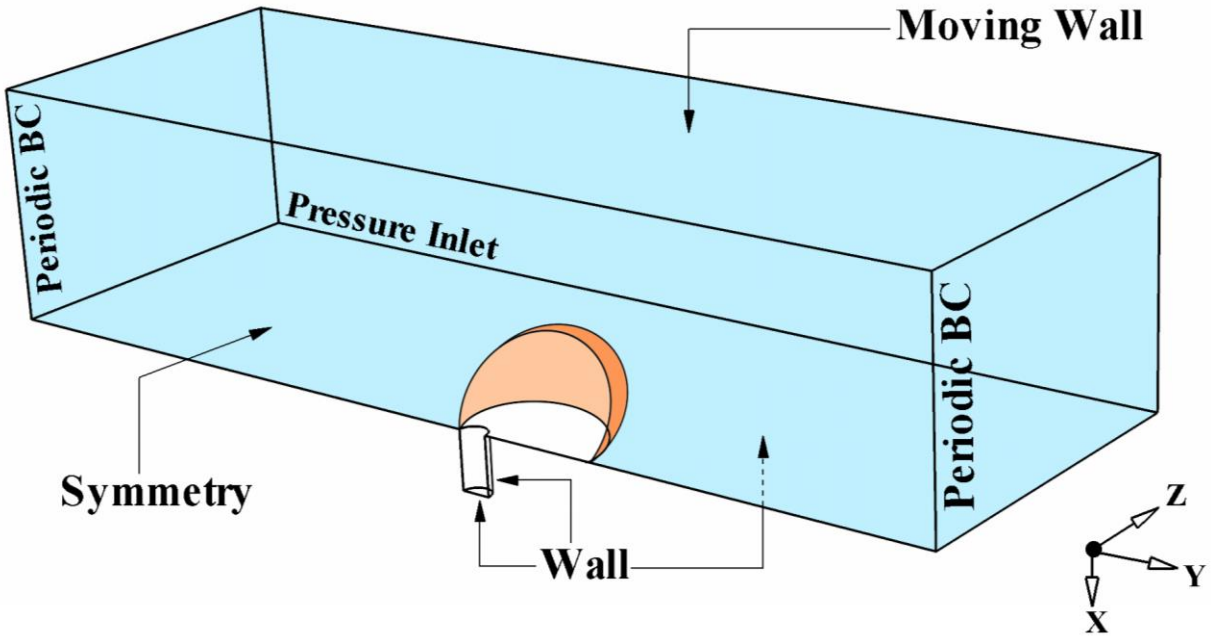

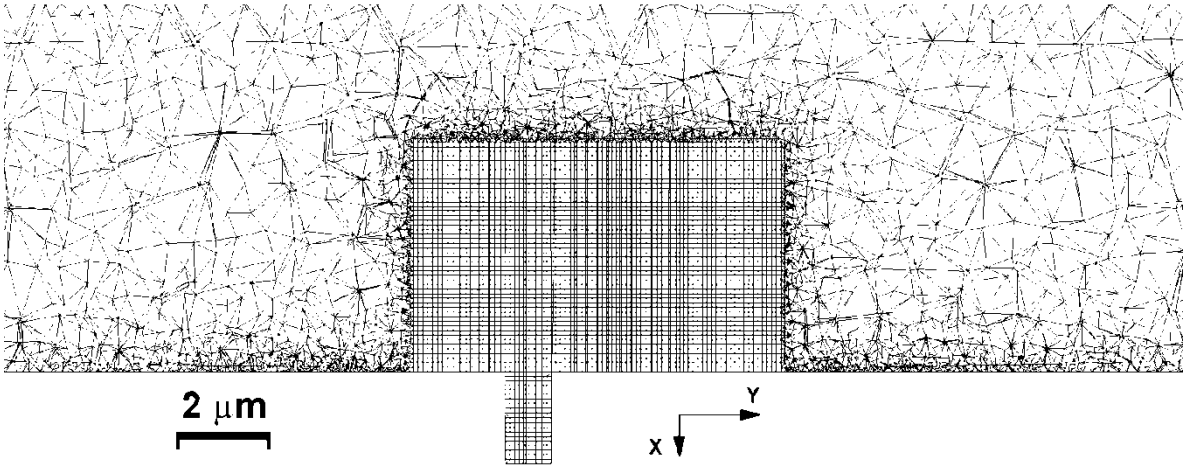

- Droplet already deposited on the pore.
- Bottom of pore is blocked.
- Symmetry boundary condition solves half of the domain. As a result saves time.
- Moving top wall generates linear shear flow.
- A hybrid mesh with coarse tetrahedral meshes away from the pore and fine hexagonal meshes near the pore is used.
- Grid independency check is confirmed

Basic parameters: r_{pore} = 0.5 μm, r_{drop} = 2.0 μm, λ = 1, σ = 19.1 mN/m, θ = 135°

Results

❑**Part 2:**

1. Problem statement.
2. **Effect of confinement on drop dynamics.**
3. Effect of viscosity ratio on drop dynamics.
4. Effect of surface tension coefficient on drop dynamics.
5. Effect of contact angle on drop dynamics.
6. Effect of drop size on drop dynamics.

Effect of Confinement on Drop Dynamics Near Circular Pores

- ❖High channel height: high computational cost.
- ❖Low channel height: not purely unconfined.
- ❖Optimum channel height?
- ❖Highly confined droplet elongates more.
- ❖Higher confinement -> lower breakup capillary number.
- ❖Optimum confinement ratio ~ 0.428

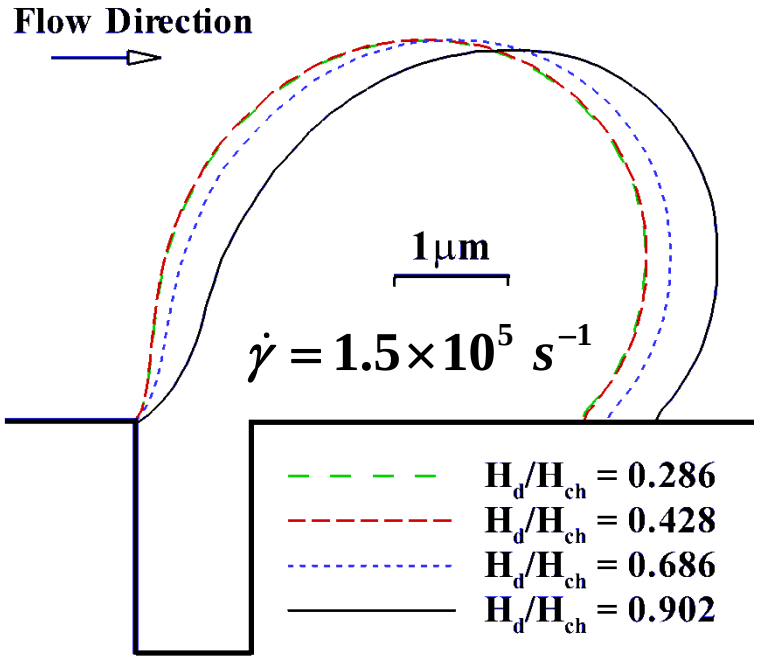

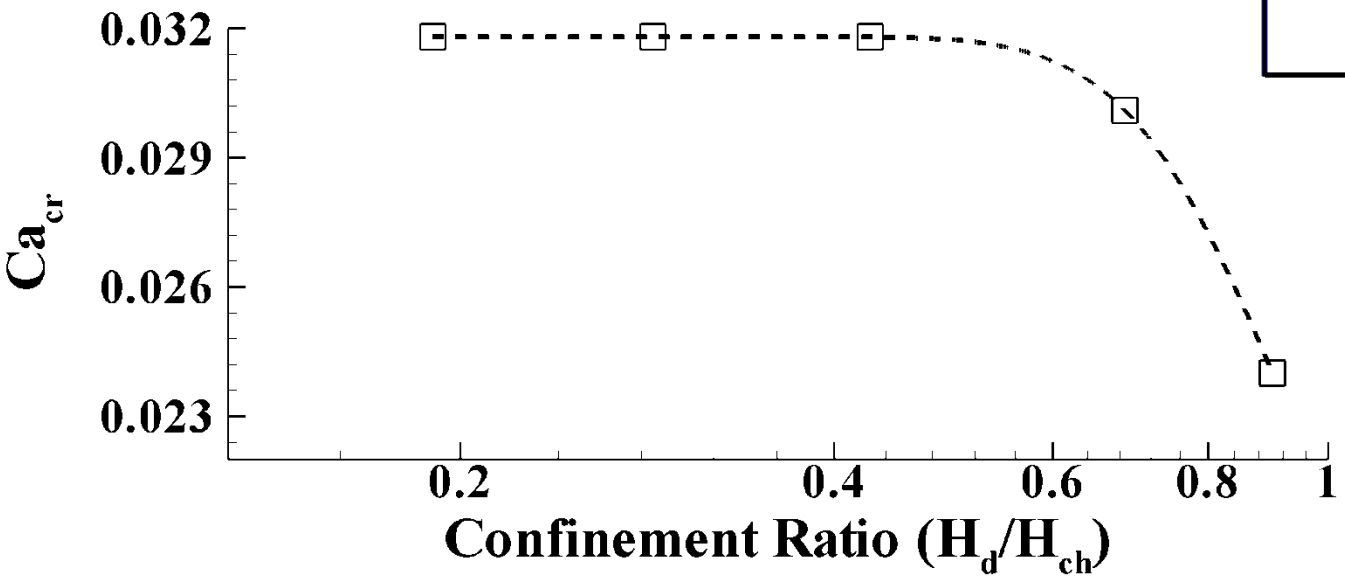

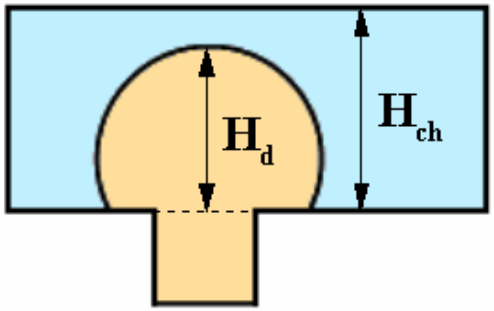

r_{pore} = 0.5 μm, r_{drop} = 2.0 μm, λ = 1, σ = 19. 1 mN/m, θ = 135°

Results

❑**Part 2:**

1. Problem statement.
2. Effect of confinement on drop dynamics.
3. **Effect of viscosity ratio on drop dynamics.**
4. Effect of surface tension coefficient on drop dynamics.
5. Effect of contact angle on drop dynamics.
6. Effect of drop size on drop dynamics.

Effect of Viscosity Ratio on Breakup Time of the Droplet

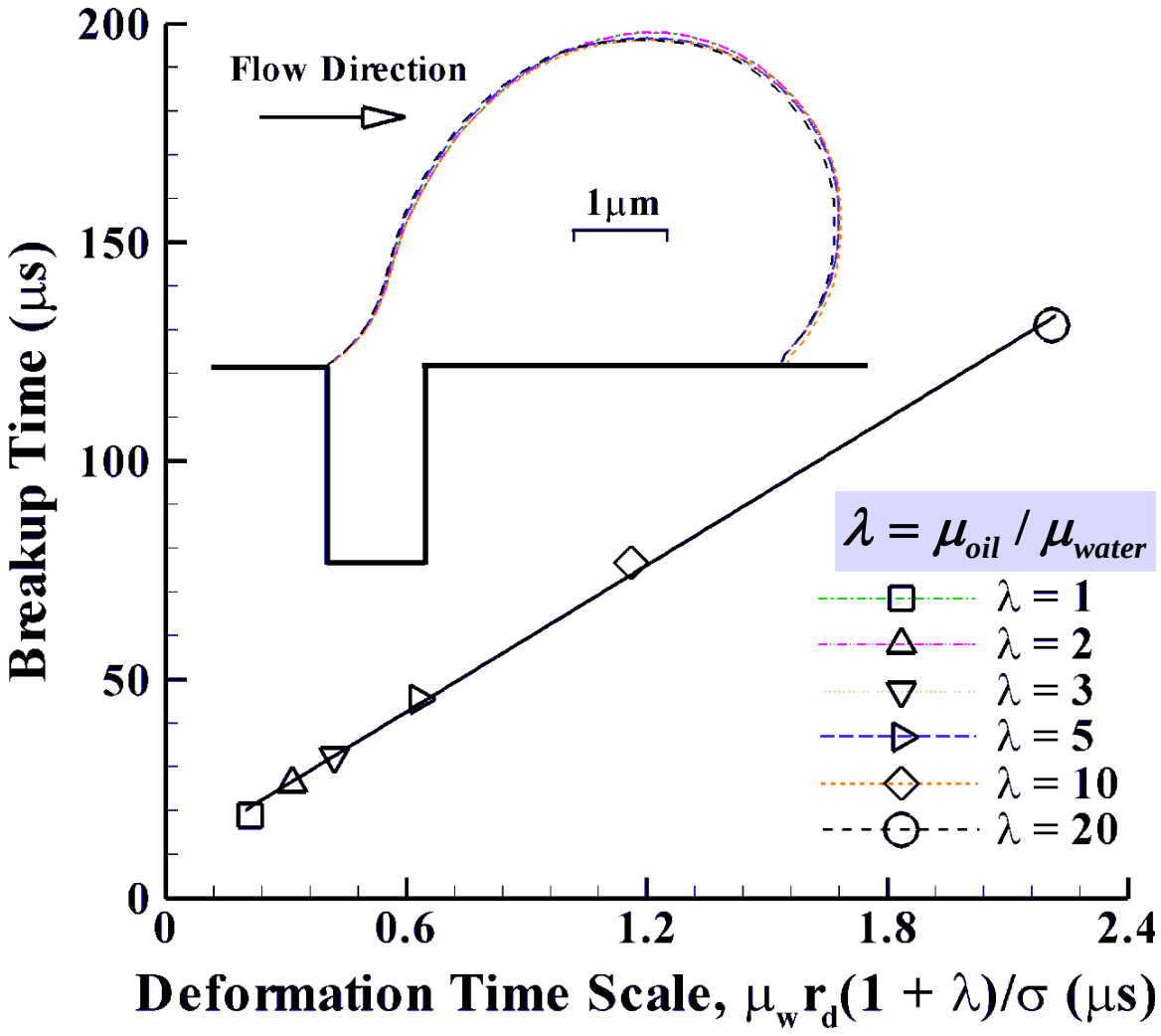

- Deformation time scale: measure of drop deformation time.
- Solid body -> infinite deformation time scale.
- Computed breakup time increases with viscosity ratio.
- Drop profiles at breakup match very closely (self-similarity).

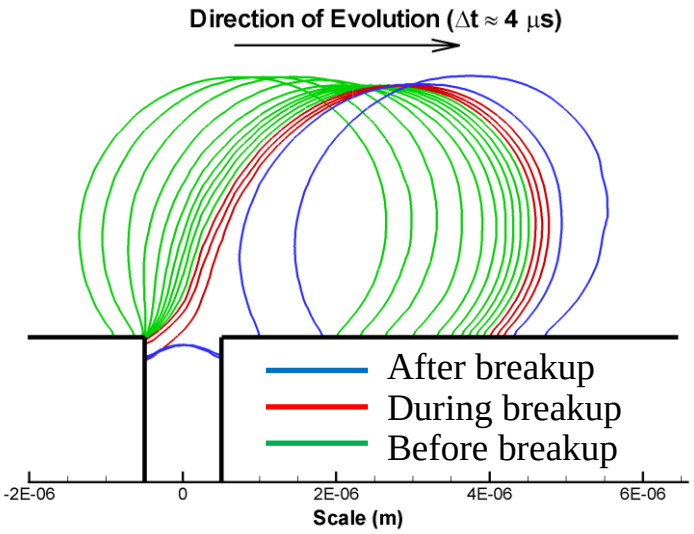

r_{pore} = 0.5 μm, r_{drop} = 2.0 μm, σ = 19.1 mN/m, θ = 135°

Effect of Viscosity Ratio on Drop Dynamics Near Circular Pores

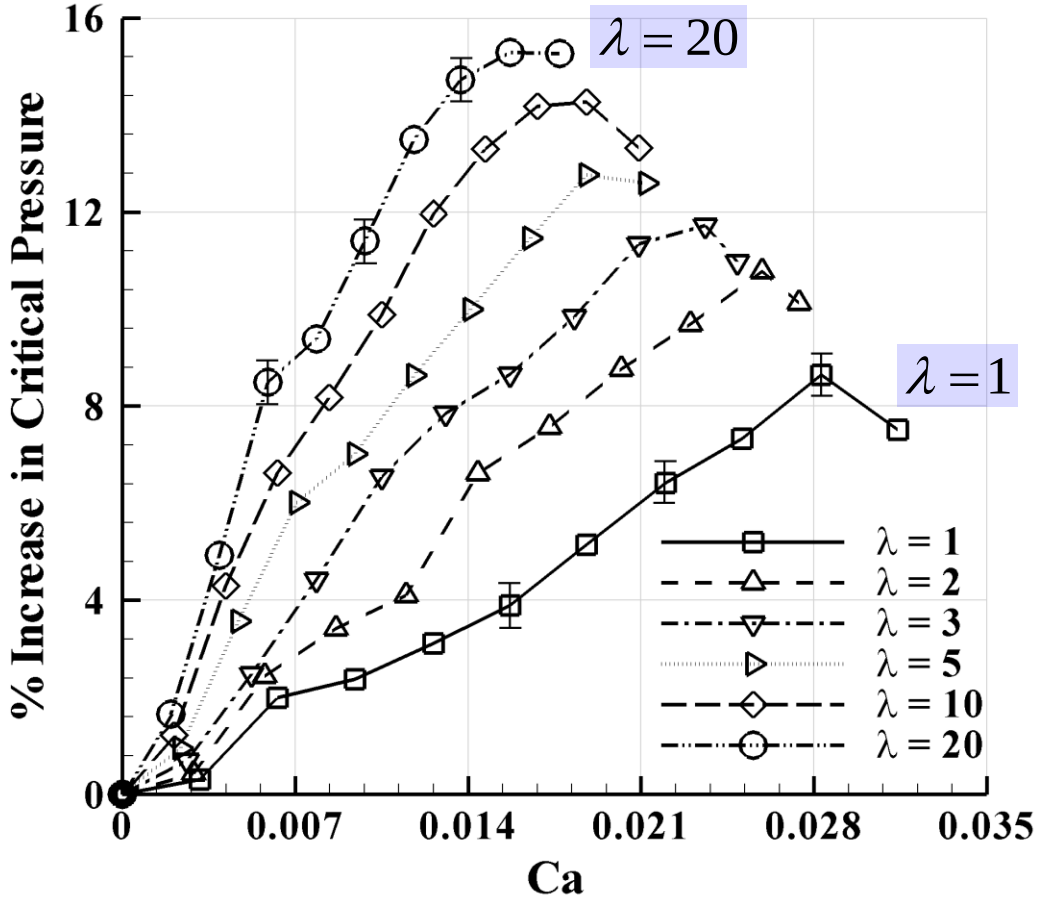

r_{pore} = 0.5 μm, r_{drop} = 2.0 μm, σ = 19.1 mN/m, θ = 135°

$$\lambda = \mu_{oil} / \mu_{water}$$

$$Ca = \frac{\mu \dot{\gamma} r_d}{\sigma}$$

$$\%IncP_{crit} = (P_{crit} - P_{crit_0}) / P_{crit_0} \times 100$$

- With increasing capillary number *Ca* critical permeation pressure increases.
- High viscosity ratio = high critical pressure.
- Higher viscosity ratio = easier breakup.
- Droplets with low viscosity ratio should be avoided for emulsification.
- Increasing *Ca* increases deformation.

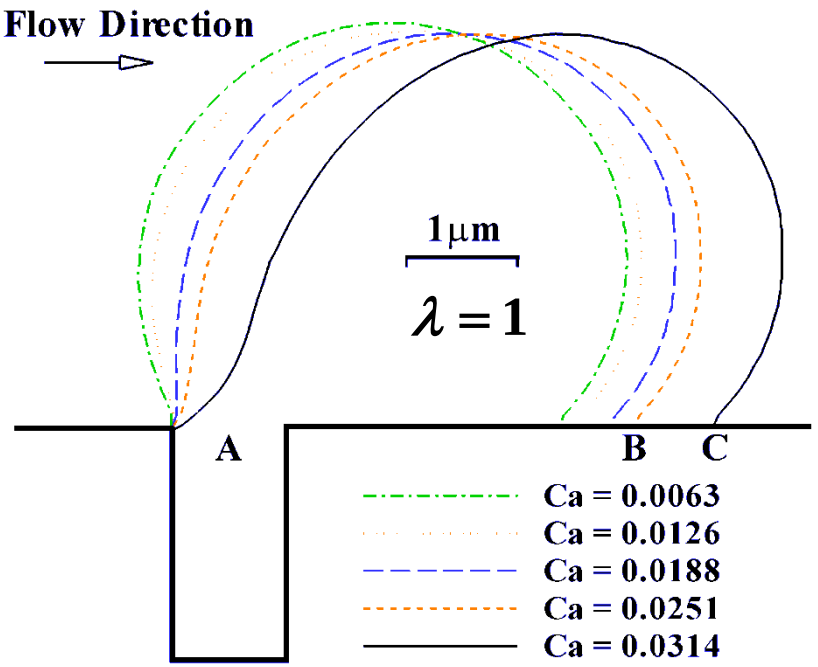

Self-similarity of the Drop Behavior for any Viscosity Ratio

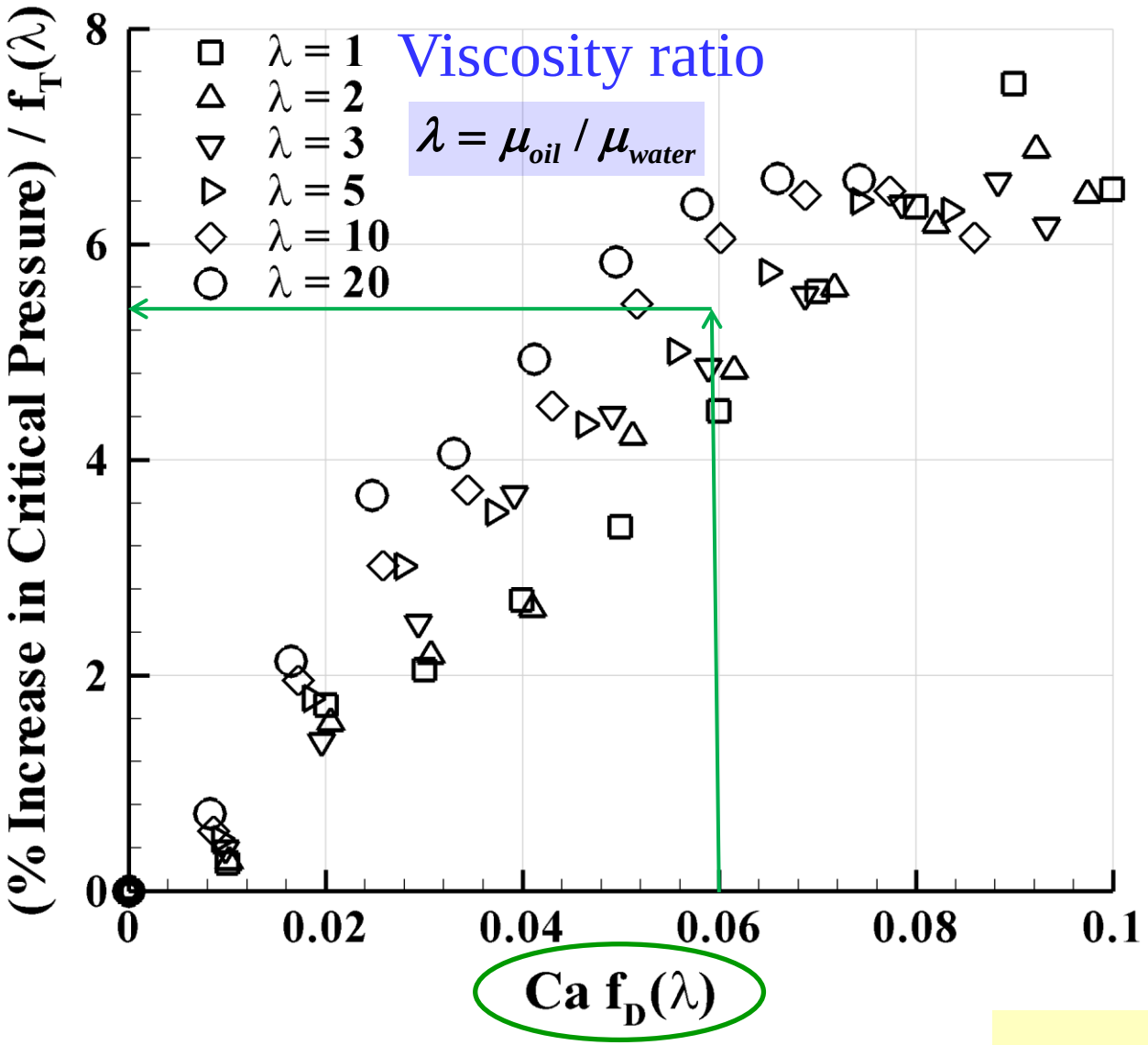

r_{pore} = 0.5 µm, r_{drop} = 2.0 µm, σ = 19.1 mN/m, θ = 135°

❖ Drops with different viscosity ratio behave similarly.

❖ Capillary number is multiplied by $f_D(\lambda)$ because highly viscous drops break at lower shear rates.

❖ Critical pressure is divided by $f_T(\lambda)$ because highly viscous drops have higher critical pressure.

$$Ca_{cr} \times f_D(\lambda) \propto \frac{1}{\bar{r}}$$

$$(P_{cr} - P_{cr_0}) / f_T(\lambda) \propto \frac{\sigma \bar{r} Ca}{r_p}$$

$$f_D(\lambda) = \frac{2 + 4.5\lambda}{1 + 1.05\lambda}$$

$$f_T(\lambda) = \frac{2.19\lambda}{1 + 0.90\lambda}$$

Results

- **Part 2:**

1. Problem statement.
2. Effect of confinement on drop dynamics.
3. Effect of viscosity ratio on drop dynamics.
4. **Effect of surface tension coefficient on drop dynamics.**
5. Effect of contact angle on drop dynamics.
6. Effect of drop size on drop dynamics.

Breakup time of droplet for different surface tension coefficients

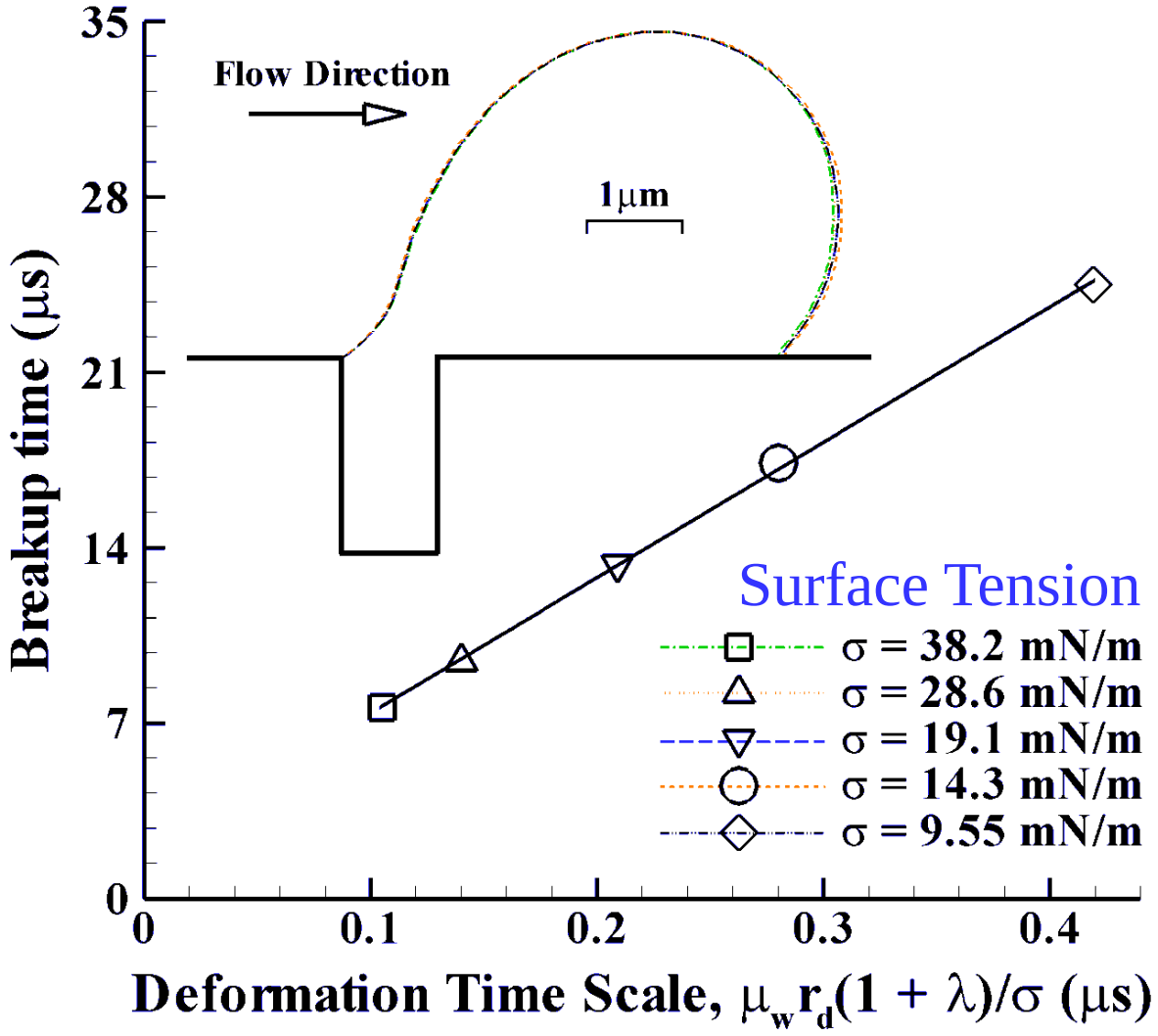

r_{pore} = 0.5 μm, r_{drop} = 2.0 μm, λ = 1, θ = 135°

- Deformation time scale decreases with surface tension.
- Breakup time linearly increases with deformation time scale.
- Drops with higher surface tension breakup faster.
- Drop profiles at breakup match exactly (self-similarity).

Deformation to steady state	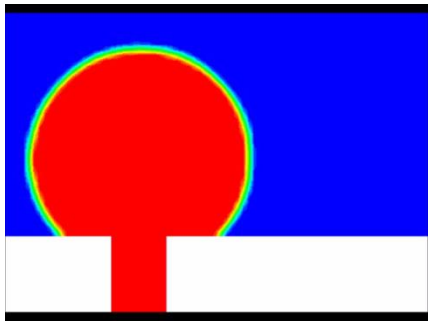
Quasi steady breakup	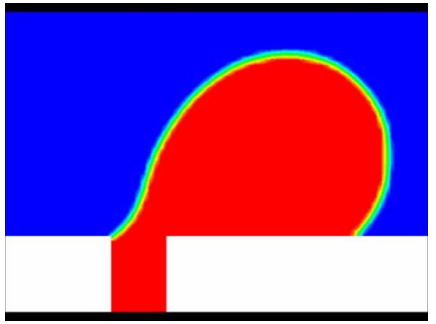

Effect of Surface Tension on Drop Dynamics Near Circular Pores

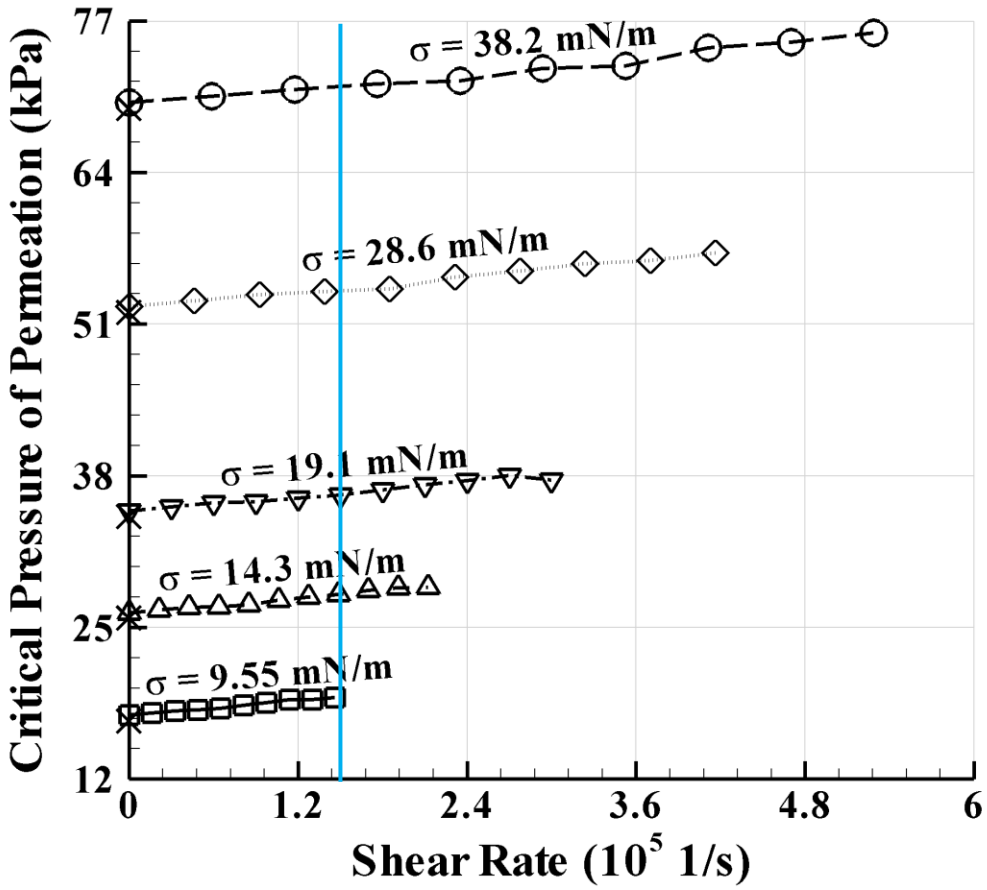

r_{pore} = 0.5 μm, r_{drop} = 2.0 μm, λ = 1, θ = 135°

Nazzal & Wiesner, (1996)

$$P_{crit} = 2\gamma \frac{\cos(\theta)}{r_{pore}} \times \left[1 - \left\{ \frac{2 + 3\cos\theta - \cos^3\theta}{4\left(\frac{r_{drop}}{r_{pore}}\right)^3 \cos^3\theta - (2 - 3\sin\theta + \sin^3\theta)} \right\}^{1/3} \right]$$

- Surface tension resists external forces (pressure, shear stress, etc.).
- Increasing surface tension coefficient increases critical pressure of permeation.
- Drops with high surface tension break at higher shear rates.
- Microfiltration -> high surface tension.

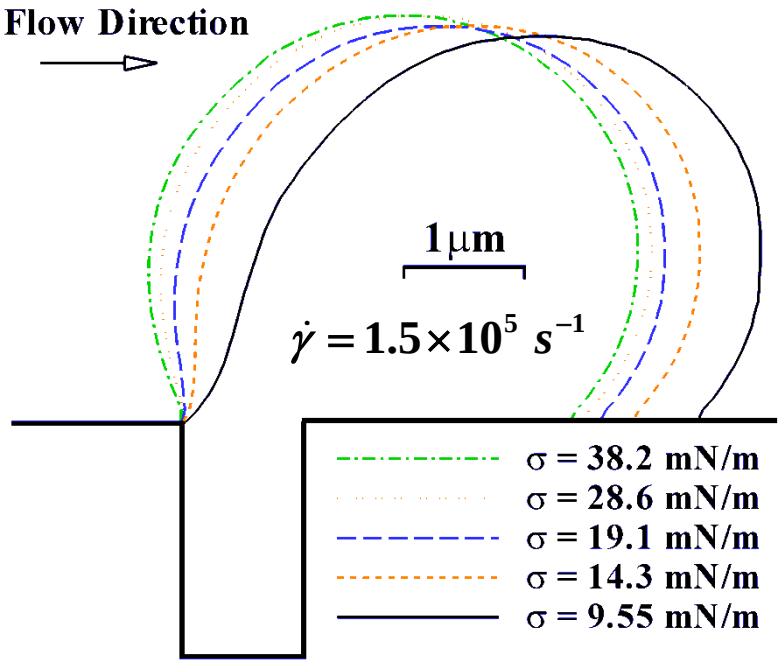

Self-similarity of the Drop Behavior for any Surface Tension

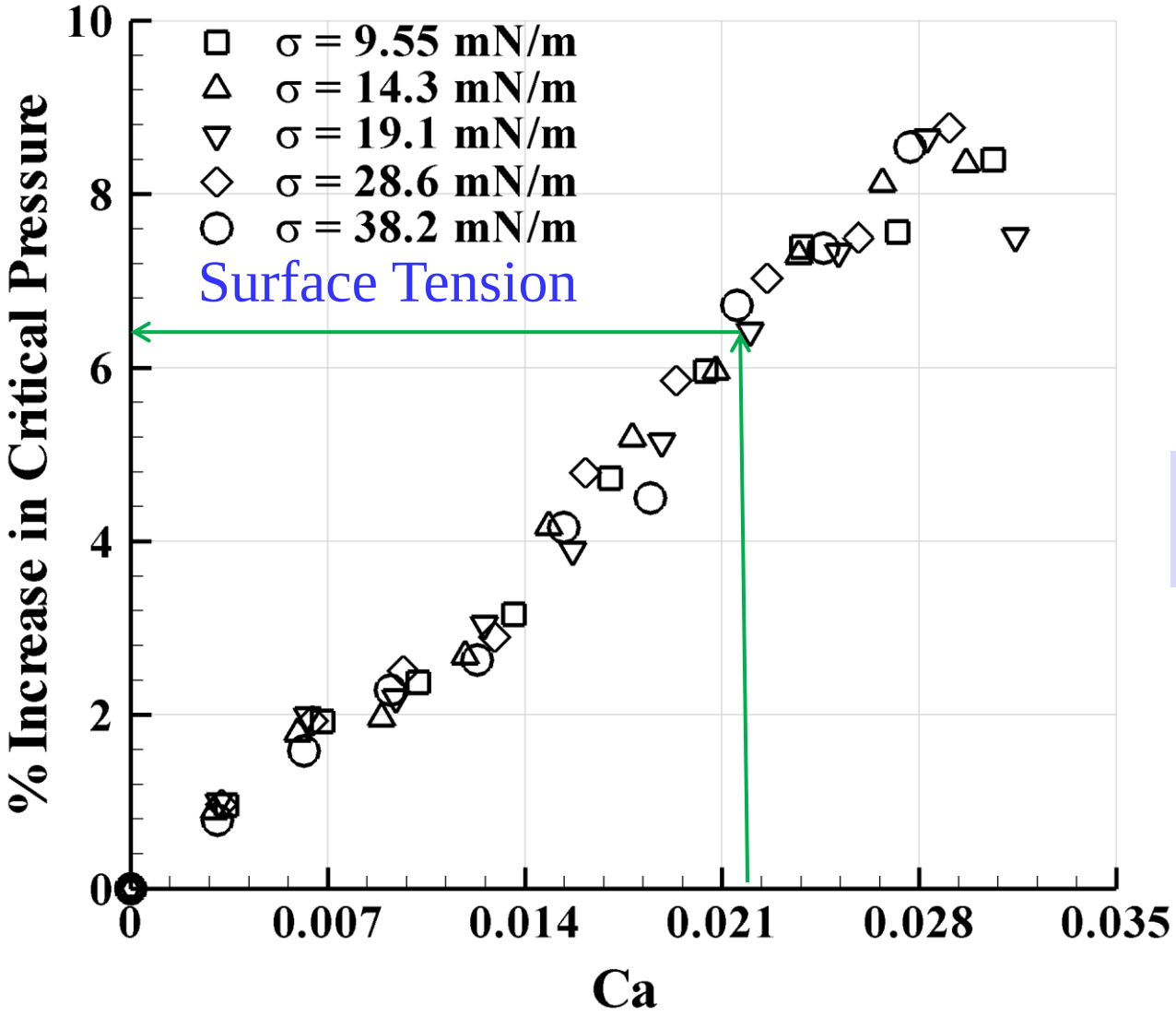

r_{pore} = 0.5 μm, r_{drop} = 2.0 μm, λ = 1, θ = 135°

❖ Dividing *Ca* and P_{cr} by the surface tension coefficient makes results independent from surface tension.

❖ Breakup at $Ca \approx 0.032$.

$$\%IncP_{crit} = \frac{(P_{crit} - P_{crit_0})}{P_{crit_0}} \times 100$$

$$P_{crit_0} \propto \sigma$$

$$Ca = \frac{\mu \dot{\gamma} r_d}{\sigma}$$

Results

- **Part 2:**

1. Problem statement.
2. Effect of confinement on drop dynamics.
3. Effect of viscosity ratio on drop dynamics.
4. Effect of surface tension coefficient on drop dynamics.
5. **Effect of contact angle on drop dynamics.**
6. Effect of drop size on drop dynamics.

Effect of Contact Angle on Drop Dynamics Near Circular Pores

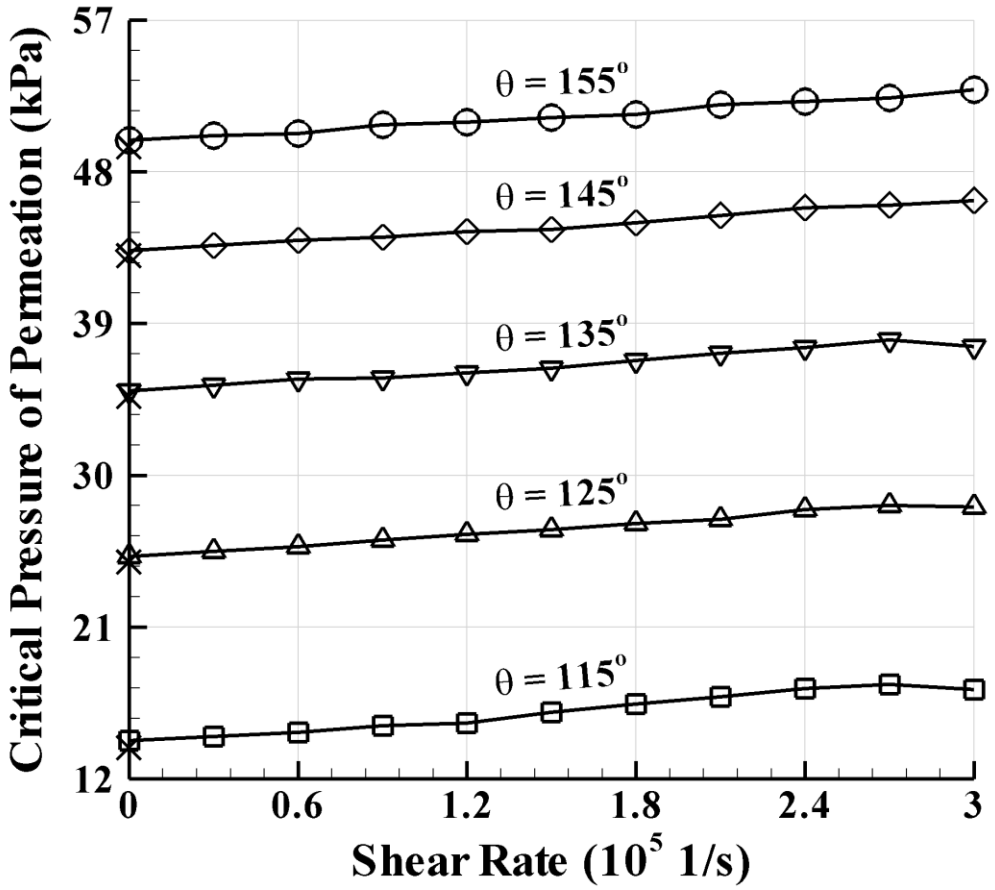

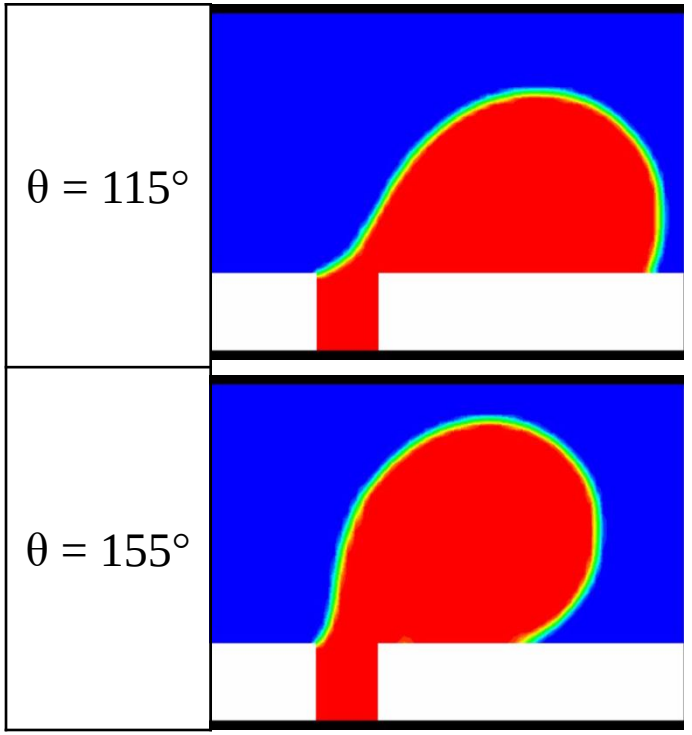

❖Increasing contact angle increases the critical pressure of permeation.

❖Breakup shear rate is roughly independent of contact angle.

❖Contact angles of 115 degrees results in a 21% increase in critical pressure before breakup while 155 increases only 6%.

r_{pore} = 0.5 μm, r_{drop} = 2.0 μm, λ = 1, σ = 19.1 mN/m

Nazzal & Wiesner, (1996)

$$P_{crit} = 2\gamma \frac{\cos(\theta)}{r_{pore}} \times \left[1 - \left\{ \frac{2 + 3\cos\theta - \cos^3\theta}{4\left(\frac{r_{drop}}{r_{pore}}\right)^3 \cos^3\theta - (2 - 3\sin\theta + \sin^3\theta)} \right\}^{1/3} \right]$$

Pressure Increase vs. Capillary Number for Different Contact Angles

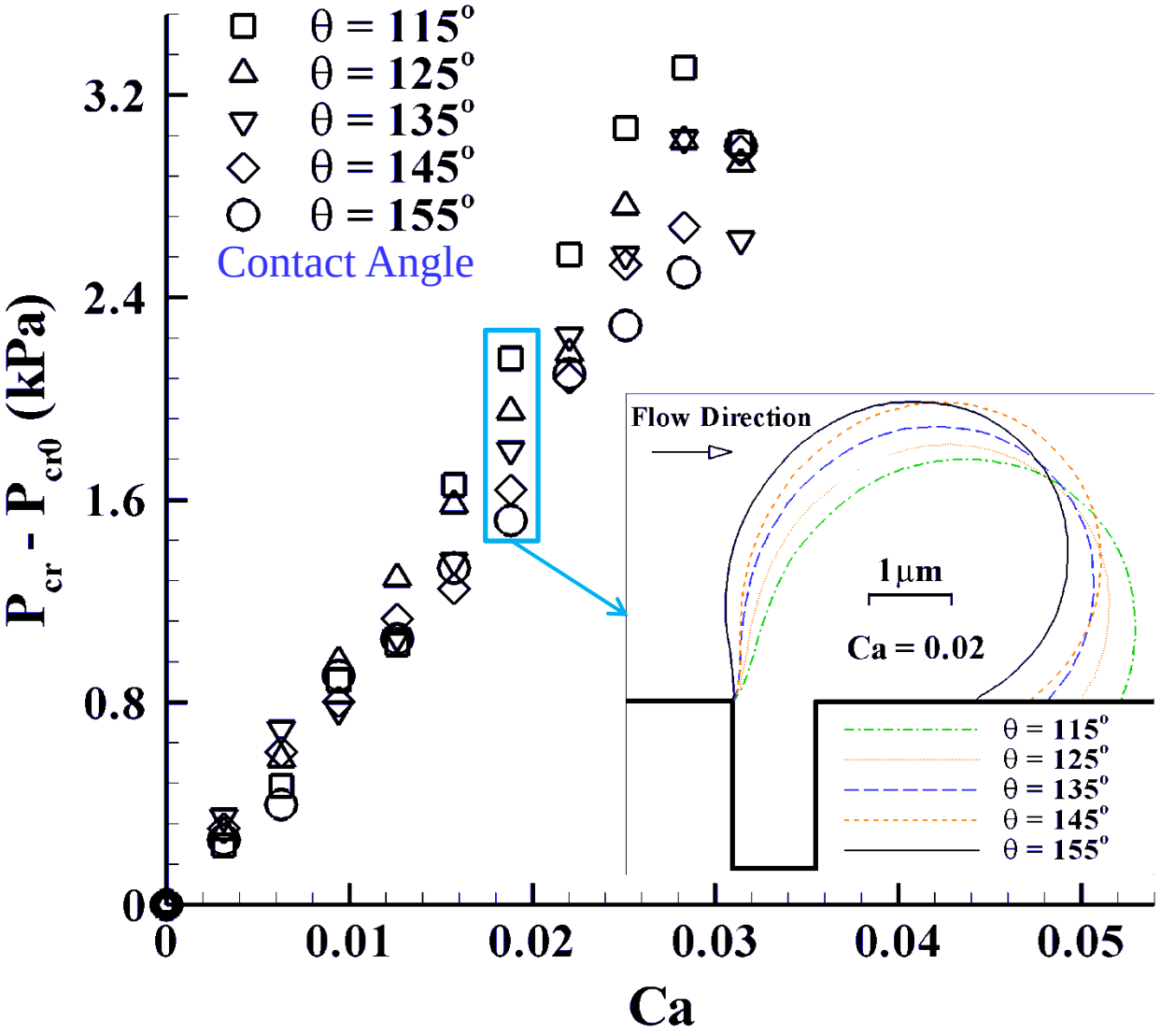

r_{pore} = 0.5 μm, r_{drop} = 2.0 μm, λ = 1, σ = 19.1 mN/m

❖Increase in critical pressure roughly independent of contact angle.

❖Lower contact angle drops are able to elongate more.

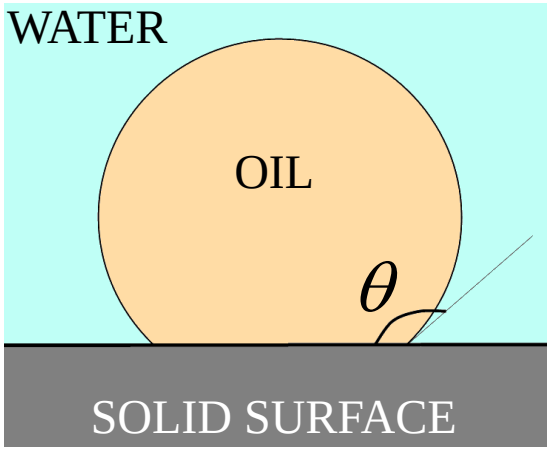

$$Ca = \frac{\mu \dot{\gamma} r_d}{\sigma}$$

$$T = f_T(\lambda)\pi\mu\dot{\gamma}r_d^{\,3}$$

Results

❑**Part 2:**

1. Problem statement.
2. Effect of confinement on drop dynamics.
3. Effect of viscosity ratio on drop dynamics.
4. Effect of surface tension coefficient on drop dynamics.
5. Effect of contact angle on drop dynamics.
6. **Effect of drop size on drop dynamics.**

Effect of Drop size on Entry Dynamics Near Circular Pores

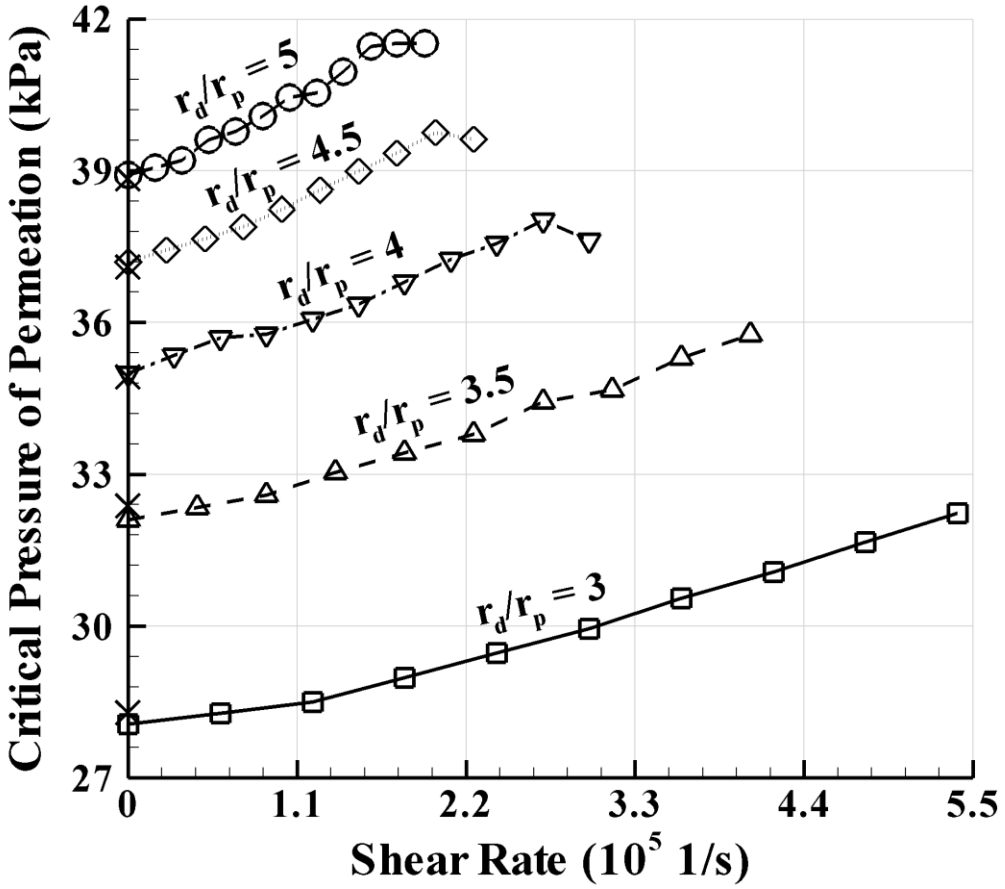

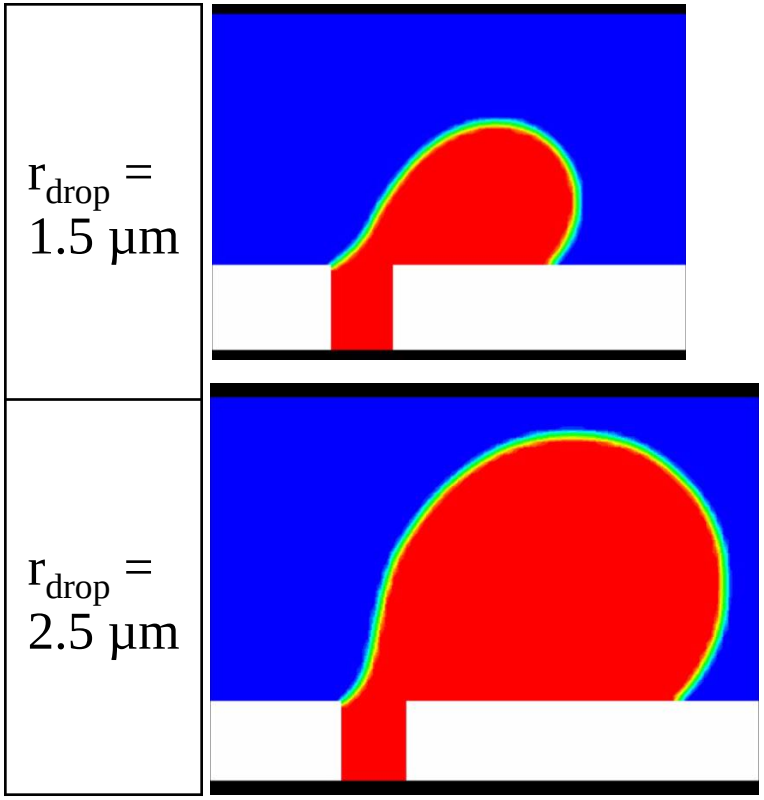

r_{pore} = 0.5 µm, λ = 1, σ = 19.1 mN/m, θ = 135°

Nazzal & Wiesner, (1996)

$$P_{crit} = 2\gamma \frac{\cos(\theta)}{r_{pore}} \times \left[1 - \left\{ \frac{2 + 3\cos\theta - \cos^3\theta}{4\left(\frac{r_{drop}}{r_{pore}}\right)^3 \cos^3\theta - (2 - 3\sin\theta + \sin^3\theta)} \right\}^{1/3} \right]$$

- Larger drops: higher critical pressure.
- Larger drops: lower breakup shear rate.
- Increase in critical pressure before breakup is higher for smaller droplets.
- Increase in critical pressure is higher for larger drops for the same shear rate.

Self-similarity of the Drop Behavior for any Drop Size

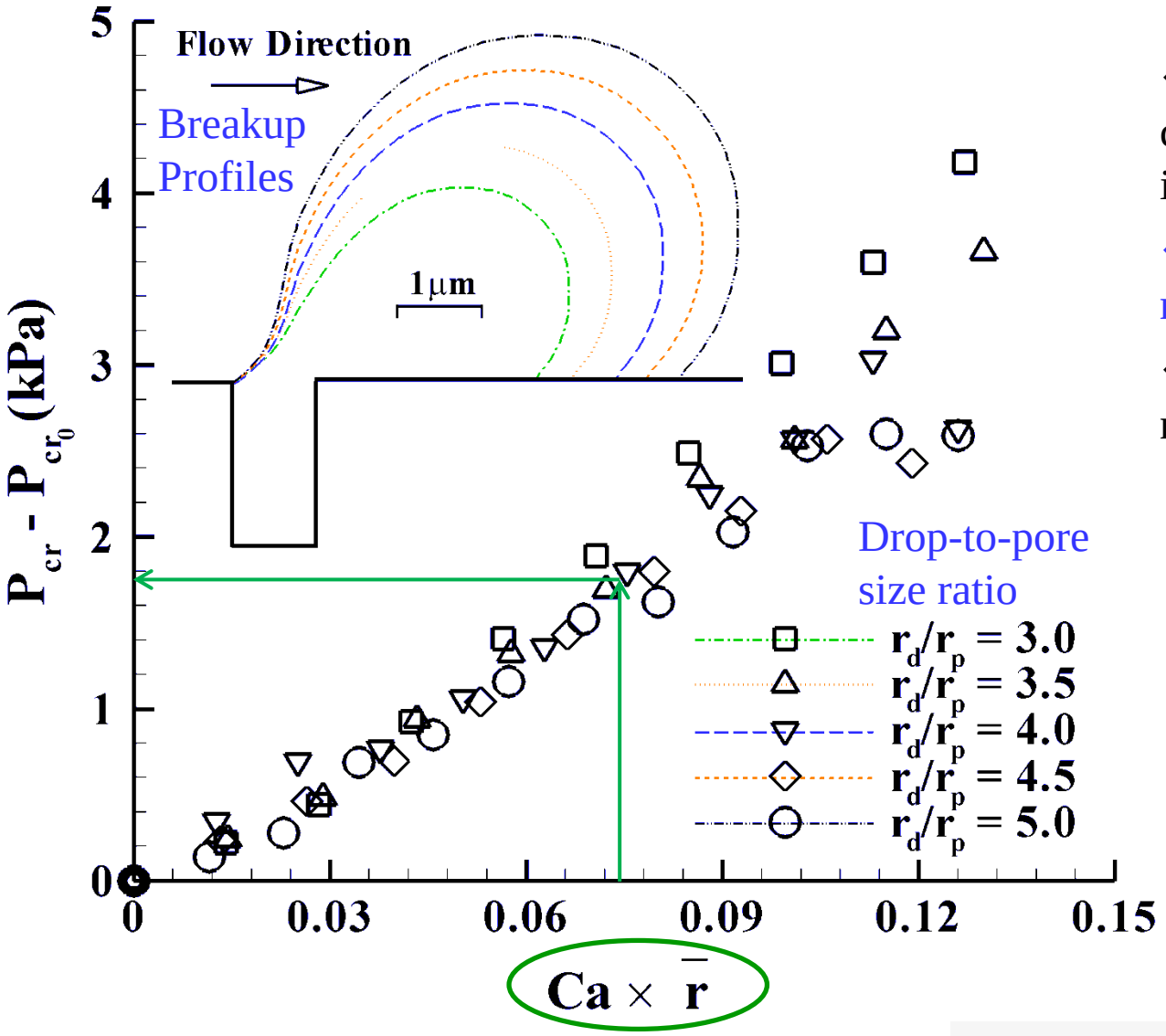

r_{pore} = 0.5 μm, λ = 1, σ = 19.1 mN/m, θ = 135°

❖ Modified breakup capillary number is independent of drop size.

❖ Smaller drops deform more near the pore.

❖New non-dimensional number identified.

$$P_{cr} - P_{cr_0} \propto \frac{f_T(\lambda)\sigma \bar{r} Ca}{r_p}$$

$$Ca_{cr} \times \bar{r} \propto f_D(\lambda)$$

$$f_D(\lambda) = \frac{2 + 4.5\lambda}{1 + 1.05\lambda}$$

$$\bar{r} = r_d / r_p$$

$$f_T(\lambda) = \frac{2.19\lambda}{1 + 0.90\lambda}$$

Summary

Increasing the parameters in green boxes improve rejection of oil

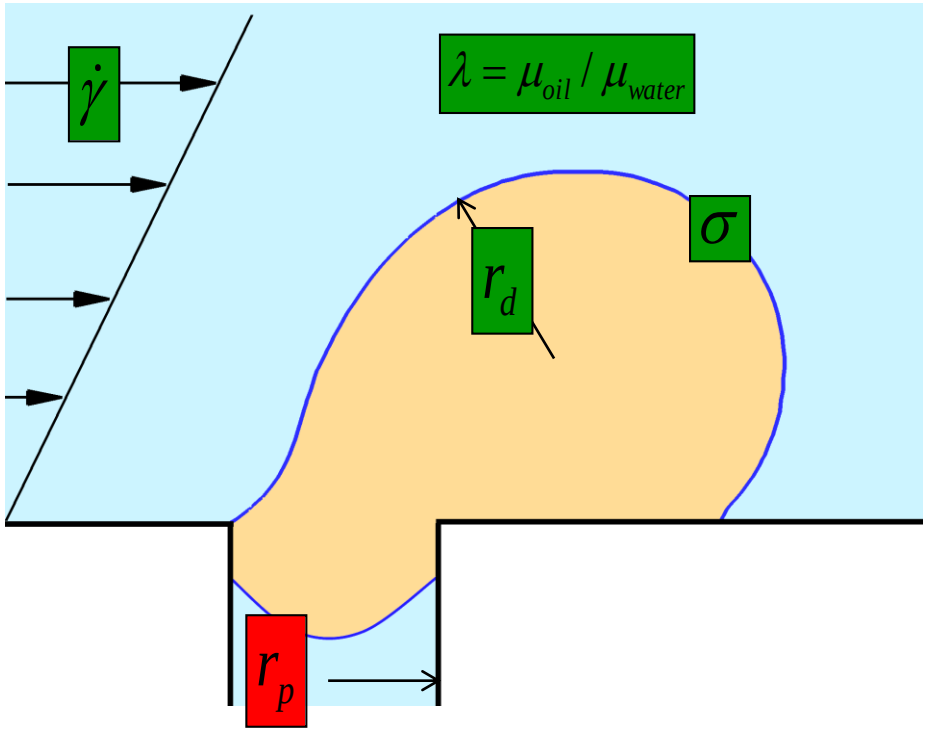

Increasing the parameters in green boxes increases chance of breakup

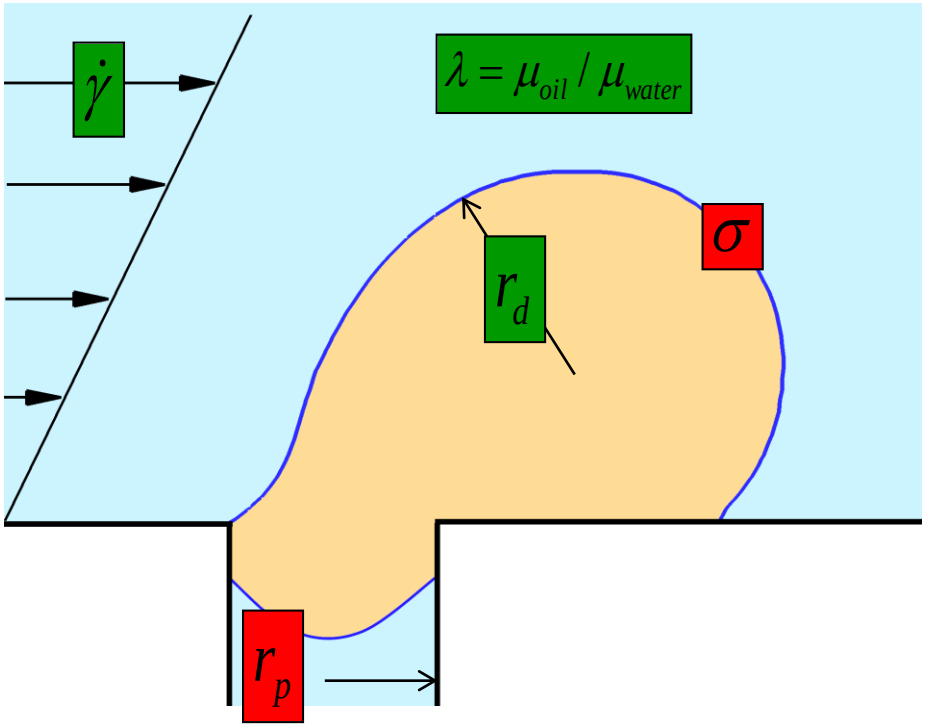

$$P_{cr} - P_{cr_0} \propto \frac{f_T(\lambda)\sigma \bar{r} Ca}{r_p}$$

$$\bar{r} = r_d / r_p$$

$$Ca_{cr} \propto \frac{1}{f_D(\lambda)\bar{r}}$$

T. Darvishzadeh, V.V. Tarabara, N.V. Priezjev, *Journal of Membrane Science*, **447**, 442-451 (2013).

T. Darvishzadeh and N.V. Priezjev, *Journal of Membrane Science*, **423-424**, 468-476 (2012).

Important Conclusions

✓A formula for calculation of critical pressure of entry of an oil film was derived and validated numerically.

✓Increasing shear flow, increases critical pressure of permeation.

✓Depending on transmembrane pressure and shear rate, a droplet near the pore of a membrane will be washes away, break, or permeate the pore.

✓Confined drops break at lower shear rates compared to unconfined drops.

✓Critical pressure for crossflow microfiltration increases with viscosity ratio, surface tension coefficient, and drop size.

✓Increasing shear rate, viscosity ratio, and size of the drop increases chance of breakup.

✓Increasing surface tension coefficient decreases chance of breakup.

✓New dimensionless variables were introduced that result in solutions independent of various parameters.

Proposed Future Work

Numerical simulation of a droplet on a membrane surface with hydrophobicity gradient.

- Constant contact angle ($\theta = 137^o$).
- Droplet pulled towards the pore due to the induced flow.

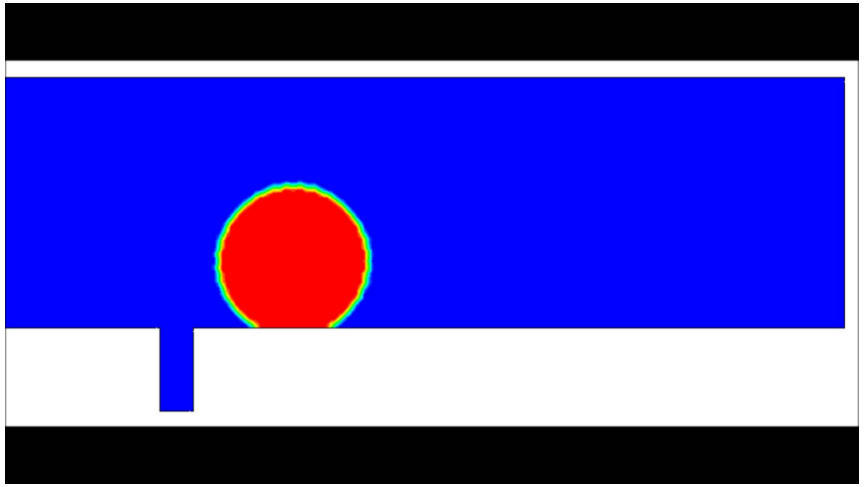

- Linear contact angle gradient along the membrane surface.
- $\theta = 150^o$ at pore entrance.
- $\theta = 70^o$ at far right side.
- Droplet driven away from the pore despite the induced flow towards the pore.

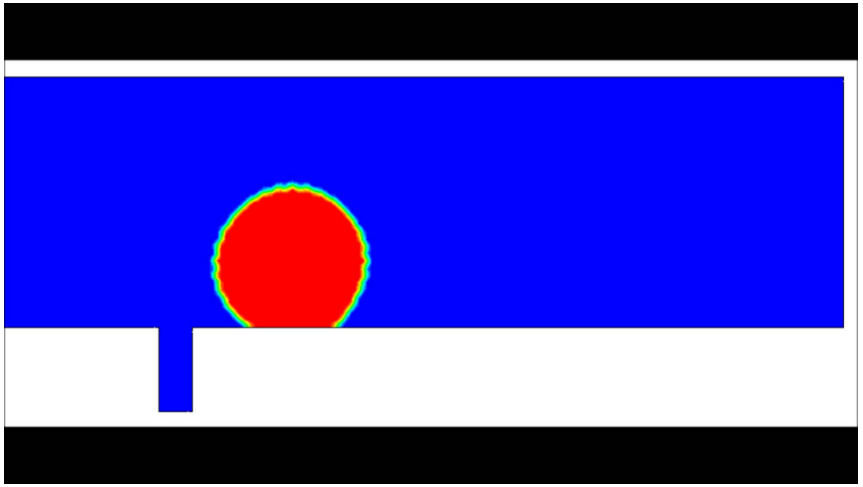

r_{pore} = 0.2 µm, r_{drop} = 0.9 µm, λ = 2.45, σ = 19.1 mN/m, ΔP = -70 kPa

Proposed Future Work (continued)

r_{pore} = 5 µm, r_{drop} = 33 µm, λ = 1, σ = 19.1 mN/m, θ = 180°, ΔP_{pore} = -10 kPa, ΔP_{lat} = 1 kPa

- Droplet interaction with multiple pores.
- Lateral pressure driven flow.
- Droplet released upstream.

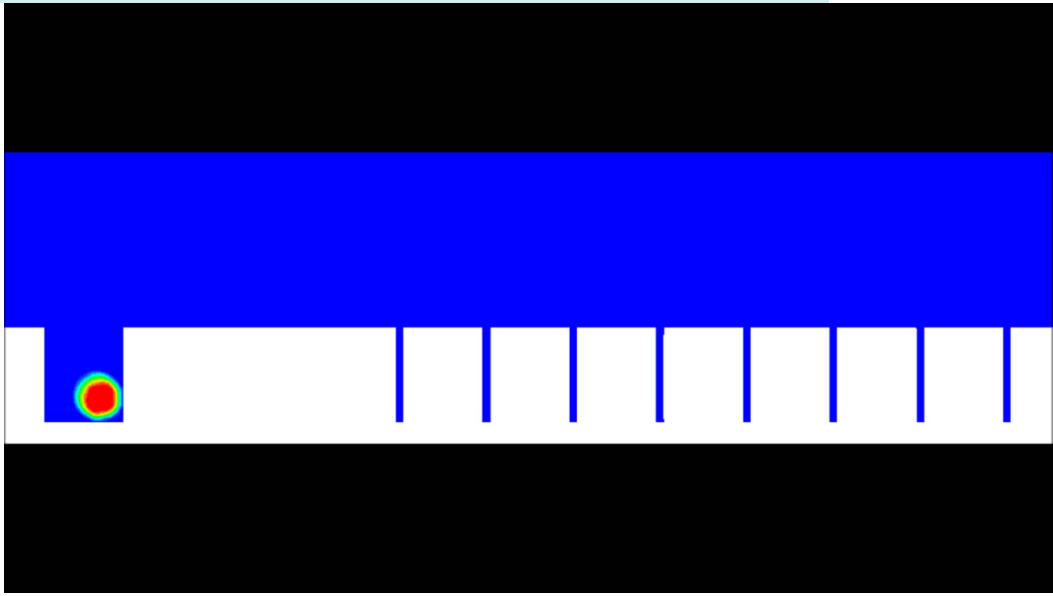

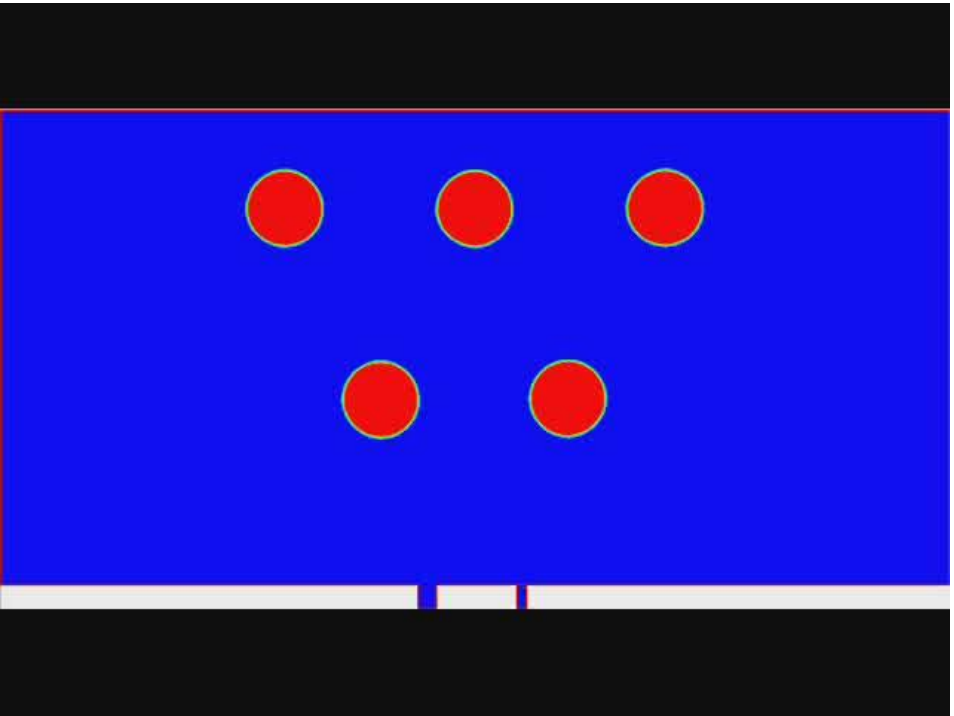

- Multiple droplets interacting with pores of different size.
- Constant transmembrane pressure.
- Higher flow rate through larger pore.
- Drops migrate towards larger pore.

r_{pore_large} = 0.1 µm, r_{pore_small} = 0.05 µm, r_{drop} = 0.4 µm, λ = 2.45, σ = 19.1 mN/m, θ = 180°, ΔP_{pore} = -150 kPa

Proposed Future Work (continued)

Droplet on slotted pore.

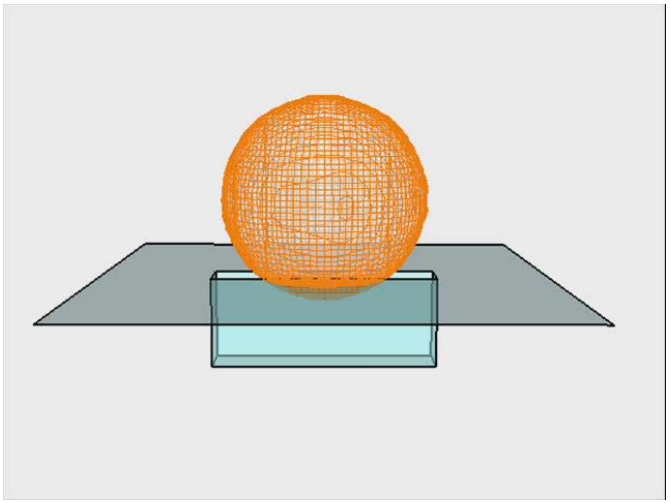

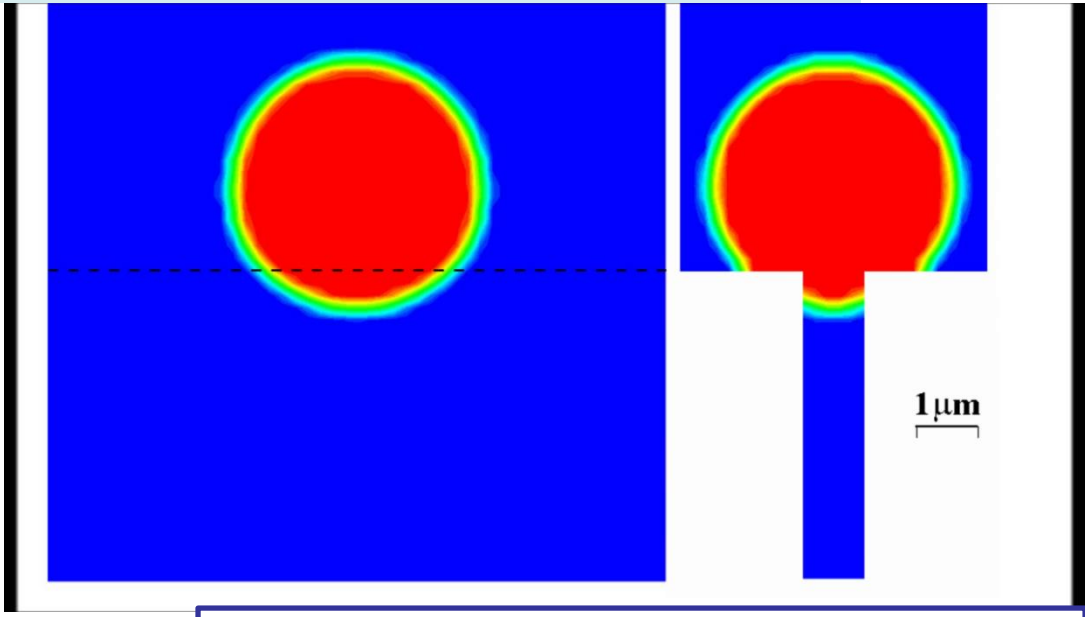

a = 1 µm, b = ∞, r_{drop} = 2 µm, λ = 1, σ = 19.1 mN/m,
θ = 135°, ΔP_{pore} = -38 kPa

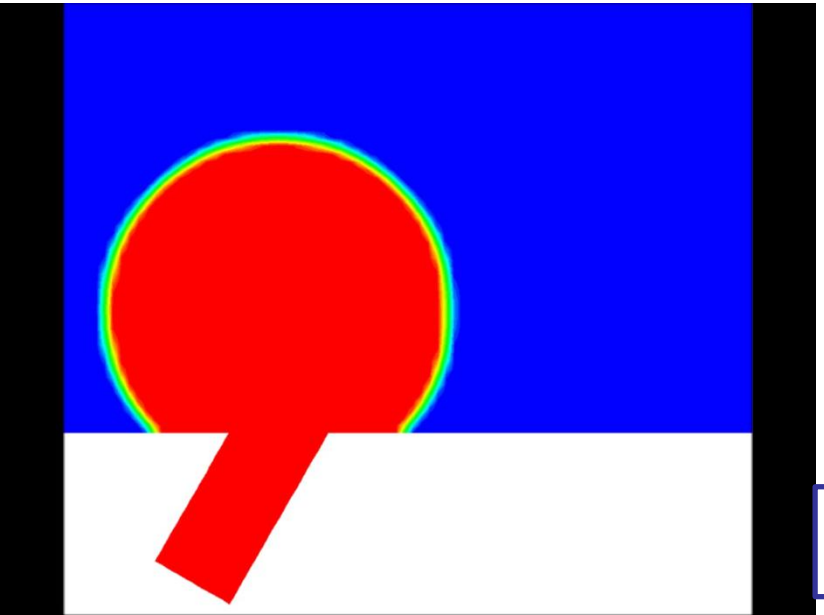

- Droplet on inclined pore.
- Hypothesis: critical pressure increases by increasing inclination angle.

r_{pore} = 0.5 µm, r_{drop} = 2 µm, θ_{pore} = 30°, λ = 1,
σ = 19.1 mN/m, θ = 135°, Shear = 5×10^5 s^{-1}

Acknowledgements

PhD Advisor

Nikolai Priezjev

PhD Committee Members:

Volodymyr Tarabara

Farhad Jaberi

Andre Benard

Funding and Support:

MSU Foundation

National Science Foundation

MSU High Performance Computing Center